

# Comparative Analysis of Holographic Dark Energy Models in $f(R, T^2)$ Gravity

M. Sharif<sup>1,2\*</sup>, M. Zeeshan Gul<sup>3,4,1†</sup> and I. Hashim<sup>1</sup> ‡

<sup>1</sup> Department of Mathematics and Statistics, The University of Lahore,  
1-KM Defence Road Lahore-54000, Pakistan.

<sup>2</sup> Research Center of Astrophysics and Cosmology, Khazar University,  
Baku, AZ1096, 41 Mehseti Street, Azerbaijan.

<sup>3</sup> College of Transportation, Tongji University, Shanghai 201804, China.

<sup>4</sup> Postdoctoral Station of Mechanical Engineering, Tongji University,  
Shanghai 201804, China.

## Abstract

This study investigates the Renyi Holographic dark energy, Sharma-Mittal Holographic dark energy and Generalized Holographic dark energy models in the framework of  $f(R, T^2)$  gravity, where  $R$  denotes the Ricci scalar and  $T^2$  represents the self-contraction of the stress-energy tensor. For this purpose we employed two horizons as infrared cut-offs, such as Hubble horizon and Ricci horizon. The analysis is conducted for a non-interacting scenario in a spatially flat Friedmann-Robertson-Walker universe. By considering a specific form of this modified gravity, we reconstruct the corresponding gravitational models based on these selected dark energy formulations. Additionally, a stability analysis is performed for all cases and the evolution of the equation of state parameter is examined. Our finding indicates that the reconstructed  $f(R, T^2)$  models effectively describe both the phantom and

---

\*msharif.math@pu.edu.pk

†mzeeshangul.math@gmail.com, zeeshan.gul@khazar.org

‡imran.hashim@math.uol.edu.pk

quintessence phases of cosmic evolution, aligning with the observed accelerated expansion of the universe. This study highlights the deep interconnections between holographic dark energy models and modified gravity theories, offering valuable insights into the large scale dynamics of the cosmos.

**Keywords:** Reconstruction technique; Modified theory; Dark energy models; Stability.

**PACS:** 04.50.Kd; 98.80.-k; 95.36.+x.

## 1 Introduction

Einstein general relativity (GR) made a significant shift in understanding of gravitational interactions by providing a geometric interpretation of gravity. It explains and works accurately to study many phenomena in the universe and has passed the solar system tests. However, GR faces certain challenges including the singularity inside the black hole, have caused researcher to modify GR. Modified gravitational theories are used as an alternate proposals to solve foundational questions while explaining dark energy (DE) as well as the cosmic accelerated expansion and numerous significant astronomical observations. These innovative theories add new features in the form of curvature invariants or the geometric components in the Einstein-Hilbert action. These modifications give comprehensive explanation to cosmic acceleration without the need of exotic energy components. The  $f(R)$  gravity, [1] which is one of the simplest extension to GR, is a model in which the Ricci scalar is replaced with its function in the Einstein-Hilbert action. A comprehensive discussion of this theory and its cosmological implications can be found in [2]. Various alternative theories and their observational constraints are examined in [3]-[21].

The emergence of singularities is considered as a curial problem associated with GR, in particular at higher curvature regimes. To overcome these problems, an innovative approach introduces generalization of GR, known as the  $f(R, T^2)$  theory or energy-momentum squared gravity (EMSG), offering a compelling alternative by introducing a correction term that involves the contraction of the energy-momentum tensor  $T^2 = T^{\xi\eta}T_{\xi\eta}$  [22]. This novel framework explores the dynamics of spacetime in the presence of matter and introducing additional degrees of freedom to overcome spacetime singularity. This correction term determines a nuanced interplay between geometry and

matter thus avoiding singularity. The incorporation of additional non-linear terms offers explanations for enigmatic cosmic phenomena [23]. It is worthwhile to mention here that this theory reduces to GR in vacuum with its dynamical features are visible in high curvature regimes.

Roshan and Shojaei [24] demonstrated that EMSG exhibits a bounce during the early universe, effectively addressing primordial singularity issues. Board and Barrow [25] employed a specific model in this framework to explore exact solutions which effectively demonstrate the cosmic evolution. Notably, this innovative approach has successfully passed solar system tests [26], enhancing its credibility. The growing interest in EMSG among researchers arises from its significant theoretical implications, consistency with observational data and relevance in cosmological contexts [27]-[28]. For instance, Bahamonde et al [29] found that various models in EMSG accurately capture the current evolutionary trends and acceleration of the universe. Ranjit et al [30] explored solutions for matter density and their cosmological implications. Sharif and his collaborators [31]-[36] comprehensively examined various aspects of this theory.

The enigmatic nature of DE and its role in the cosmic accelerated expansion has been a central focus in cosmology. Chattopadhyay et al [37] investigated the reconstruction of the PDE model in the framework of  $f(T, T_G)$  gravity and examined that the reconstructed model exhibits a phantom-like behavior for specific choices of model parameters. The generalized ghost PDE has also been analyzed in [38]. Jawad and Chattopadhyay [39] explored the correspondence phenomenon in the context of modified Horava-Lifshitz gravity and found that the cosmological parameters associated with the reconstructed models align with present-day observational data. Odintsov et al [40] explored specific  $f(R, G)$  models to understand their role in driving both DE-induced acceleration and the inflationary epoch. To understand the impacts of DE on the current acceleration of the cosmos, researchers have formulated various DE models [41]. However, majority of the existing models has not tackled the nature of DE. This motivates the cosmologists to pursue the novelty of a DE model grounded on the laws governing quantum gravity and particle physics. In this respect, the Holographic DE (HDE) model was introduced [42], offering a clear understanding of DE while addressing theoretical challenges in the standard cold dark matter model. In recent years, various DE models have been established to understand the accelerated cosmic expansion, each grounded in different theoretical foundations. Among these, the agegraphic DE model links the energy density

of DE to the universe age, offering an intriguing approach to cosmic evolution. Moreover, researchers have introduced novel DE models inspired by Holographic principle and multiple entropy formalisms, leading to the development of Rényi HDE (RHDE) [43], Tsallis HDE [44] and Sharma-Mittal DE (SMHDE) models [45].

The phenomenon of cosmic expansion has been explored through various DE models, including RHDE and SMHDE in the framework of loop quantum cosmology [46]. Moradpour et al [47] applied the thermodynamic approach to HDE and RHDE to study the accelerated expansion of the universe. Furthermore, different variants of HDE models have been analyzed in [48] with their implications in a D-dimensional fractal universe [49]. Anisotropic RHDE models in GR has been investigated in [50]. Sharma and Dubey [51] explored the SMHDE model in an isotropic and spatially homogeneous flat Friedmann-Robertson-Walker (FRW) universe by considering different values of the parameters with IR cutoff governed by the Hubble horizon. The accretions of variants of HDE models onto higher-dimensional Schwarzschild black hole and Morris-Thorne wormhole have been investigated in [52]. Shekh et al [53] examined the RHDE and SMDE models in  $f(\mathcal{T}, B)$  gravity (here  $\mathcal{T}$  is the torsion and  $B$  is the boundary term) using the Hubble horizon as the IR cutoff. Further studies examined the new agegraphic DE models in generalized Rastall gravity [54]. Various generalizations of the HDE paradigm have been formulated to capture different aspects of cosmic evolution [55]. Upadhyay and Dubey [56] diagnosed the Sharma-Mittal HDE through state-finder and found the transition from decelerated to accelerated expansion of the universe. The Sharma-Mittal HDE has also been investigated in the context of Brans-Dicke scalar-tensor gravity [57], where its cosmic aspects has been discussed in [58]. The study of different DE models to study the mysterious universe has been studied in non-metric theories has been studied in [59]-[61].

In this study, we investigate the application of various HDE models in the framework of  $f(R, T^2)$  gravity to examine their implications for cosmic evolution. The structure of the paper is organized as follows. In section **2**, we derive the field equations governing this modified gravity framework in the context of flat FRW universe. Sections **3** and **4** focus on the analysis of cosmic dynamics by employing the RHDE, SMHDE and GHDE models through Hubble horizon and Ricci horizon as IR cutoff, providing a comparative evaluation of their behavior. Finally, the key findings of our results are given in sections **5**.

## 2 The $f(R, T^2)$ theory

The  $f(R, T^2)$  gravity offers a significant development in theoretical physics, presenting novel opportunities to examine cosmological phenomena beyond the standard paradigm. The action of gravity theory includes the Ricci scalar and the self-contraction of the energy-momentum tensor. The corresponding action is formulated as [22]

$$\mathcal{S} = \int d^4x \left( \frac{1}{2\kappa^2} f(R, T^2) + \mathbf{L}_m \right) \sqrt{-g}. \quad (1)$$

Here, the matter Lagrangian density and determinant of metric tensor are designated by  $\mathbf{L}_m$  and  $g$  respectively, whereas,  $\kappa^2 = 1$  is the coupling constant. The corresponding field equations are derived by applying the variational principle to the action with respect to the metric tensor as

$$f_{T^2}\Theta_{\xi\eta} + R_{\xi\eta}f_R - \frac{1}{2}g_{\xi\eta}f + (g_{\xi\eta}\square - \nabla_\xi\nabla_\eta)f_R = T_{\xi\eta}, \quad (2)$$

where

$$\Theta_{\xi\eta} = -4\frac{\partial^2 \mathbf{L}_m}{\partial g^{\xi\eta}\partial g^{\varphi\beta}}T^{\varphi\beta} - 2\mathbf{L}_m(T_{\xi\eta} - \frac{1}{2}g_{\xi\eta}T) - TT_{\xi\eta} + 2T_\xi^\varphi T_{\eta\varphi}. \quad (3)$$

Here,  $f_R = \frac{\partial f}{\partial R}$ ,  $f_{T^2} = \frac{\partial f}{\partial T^2}$ ,  $\square = \nabla^\xi\nabla_\xi$  and  $\nabla_\xi$  is the covariant derivative. We consider the dust matter distribution as

$$T_{\xi\eta} = \rho \mathbb{U}_\xi \mathbb{U}_\eta, \quad (4)$$

where  $\mathbb{U}_\mu$  determines the four velocity and  $\rho$  is the energy density. Equation (3) corresponding to  $\mathbf{L}_m = \rho$  turns out to be

$$\Theta_{\xi\eta} = -2\rho(T_{\xi\eta} - \frac{1}{2}g_{\xi\eta}T) - TT_{\xi\eta} + 2T_\xi^\varphi T_{\varphi\eta}. \quad (5)$$

Rearranging Eq.(2), we have

$$G_{\xi\eta} = \frac{1}{f_R}(T_{\xi\eta} + T_{\xi\eta}^{DE}). \quad (6)$$

Here,

$$T_{\xi\eta}^{DE} = \frac{1}{2}g_{\xi\eta}(f - Rf_R) - (g_{\xi\eta}\square - \nabla_\xi\nabla_\eta)f_R - f_{T^2}\Theta_{\xi\eta}. \quad (7)$$

To explore the mysterious universe, we assume the flat FRW model as it is consistent with the cosmological principle, ensuring homogeneity and isotropy on large scales. This model is given as

$$ds^2 = dt^2 - \mathbf{a}^2(t)d\chi^2. \quad (8)$$

Here,  $d\chi^2 = dx^2 + dy^2 + dz^2$  and  $\mathbf{a}(t)$  represents the scale factor. Using Eqs.(2)-(8), the corresponding field equations are obtained as follows

$$3H^2 = \rho_{total}, \quad (9)$$

$$3H^2 + 2\dot{H} = -p_{total}. \quad (10)$$

The Hubble parameter  $H = \frac{\dot{a}}{a}$  (where dot designates the derivative with respect to time) is a significant quantity in modern cosmology that determines the cosmic expansion rate. It serves as a crucial observational tool for understanding cosmic expansion history, the nature of DE and deviations from standard gravity,  $\rho_{total} = \rho + \rho_{DE}$ ,  $p_{total} = p_{DE}$  and

$$\rho_{DE} = \frac{1}{f_R} \left[ ((1 - f_R) + \rho f_{T^2})\rho + \frac{1}{2}(f - Rf_R) - 3H\dot{R}f_{RR} \right], \quad (11)$$

$$p_{DE} = \frac{1}{f_R} \left[ \frac{1}{2}(Rf_R - f) + \ddot{R}f_{RR} + \dot{R}^2 f_{RRR} + 2H\dot{R}f_{RR} \right]. \quad (12)$$

The field equations are complex due to the multivariate functions and their partial derivatives. To simplify the analysis and obtain explicit solutions, we adopt a specific functional form for the theory as

$$f(R, T^2) = \alpha R^n + \beta T^2, \quad (13)$$

where  $\alpha$  and  $\beta$  are non-zero constants.

This functional form is motivated by both mathematical feasibility and physical relevance. Power-law extensions of the Ricci scalar have been extensively explored in modified frameworks, as they are natural generalization of GR and provide rich cosmological dynamics. The constant  $\alpha$  emerges as a coupling parameter that determines the deviation from GR, whereas,  $\beta$  plays a significant role in exploring the influence of the  $T^2$ , by introducing  $\beta$ , we can examine a spectrum of scenarios. Thus,  $\alpha$  and  $\beta$  not only shape the overall dynamics of the model but also provide a systematic way to investigate the interplay between geometry and matter. Their combined effects

enable the study of a broad class of solutions that may address outstanding problems in cosmology, such as the nature of late-time acceleration and the role of matter-induced modifications in the evolution of the universe. Using Eqs.(5) and (13) into the field equations (11) and (12), we get

$$\begin{aligned}\rho_{DE} &= \frac{1}{\alpha n R^{n-1}} \left[ -3\alpha n(n-1)H R^{n-2} \dot{R} + \rho(\beta\rho + (1 - \alpha n R^{n-1})) \right. \\ &\quad \left. + \frac{1}{2}(\beta\rho^2 - \alpha n R^n + \alpha R^n) \right],\end{aligned}\quad (14)$$

$$\begin{aligned}p_{DE} &= \frac{1}{\alpha n R^{n-1}} \left[ \alpha n(n-1)R^{n-2} \ddot{R} + \frac{1}{2} \left( -\beta\rho^2 - \alpha n R^n + \alpha R^n \right. \right. \\ &\quad \left. \left. + 2\alpha n(n-1)H\dot{R} + \alpha n(n-1)(n-2)R^{n-3} + \dot{R}^2 \right) \right].\end{aligned}\quad (15)$$

In this innovative framework, the non-conserved stress-energy tensor indicates the presence of geodesic motion of particles, leading to additional physical effects not incorporated in standard models. The resulting non-conserved stress-energy tensor is given by

$$\nabla^\xi T_{\xi\eta} = \nabla^\xi \Theta_{\xi\eta} f_{T^2} - \frac{1}{2} g_{\xi\eta} \nabla^\xi f(T^2). \quad (16)$$

Solving this equation, we have

$$\dot{\rho} + H\rho + \rho\dot{H} + 3H\rho_{DE}(1 + \omega_{DE}) = \rho^2 \dot{f}_{T^2} - 3H\rho^2 f_{T^2} - 3\dot{\rho}\rho f_{T^2}. \quad (17)$$

In the next sections, we present a reformulation of the RHDE, SMDE and GHDE models through Hubble horizon and Ricci horizon as IR cut-offs. This involves revisiting their theoretical foundations, modifying their formulations in the  $f(R, T^2)$  theory and analyzing their implications for cosmic evolution.

### 3 The Hubble Horizon

This horizon plays a significant role in gravitation and cosmology as a natural length scale that characterizes the causal structure and cosmic evolution. The expression for the Hubble horizon in terms of Hubble parameter is  $L_H = \frac{1}{H}$ , it measures the distance over which the universe expansion becomes curial in a Hubble time. Physically, it defines the growing boundary beyond which

the particles move faster than the speed of light due to the cosmic expansion. From theocratical point of view, it appears naturally in the Friedmann equations as scale relating the cosmic expansion rate to its energy density. This relationship exhibits  $L_H$  as measure of dynamical responses of spacetime to the total energy content. Specifically, in HDE models, the Hubble horizon as an IR cut-off connects large-scale cosmological dynamics with quantum field theoretic and thermodynamic principles. Moreover, the Hubble horizon is measured locally through the instantaneous expansion rate. This local character makes it particularly suitable for constructing cosmological models that aim to describe the current cosmos without requiring knowledge of its complete history or fate.

Now, we provide a detail analysis of several well-established HDE models in the background of Hubble horizon as IR cutoff. Using these models, we derive the analytical expressions for the unknown quantities in the field equations. These HDE models offer a compelling framework for explaining the late time acceleration of the universe. By examining these models, we aim to gain deep insights into the nature of DE and its implications for the evolution of the cosmic expansion.

### 3.1 Rényi Holographic Dark Energy Model

The Rényi HDE model appears from the interaction between quantum gravity and thermodynamics, providing a modified entropy. Derived from Rényi entropy, this innovative framework provides a more generalized view on the thermodynamic properties of the universe, potentially overcomes the coincidence problem. The Tsallis entropy (TE) is given as

$$\mathcal{S}_T = \frac{1}{\zeta} \sum_{j=1}^X (\mathcal{P}_j^{1-\zeta} - \mathcal{P}_j), \quad (18)$$

where  $\mathcal{P}_j$  determines the probability distribution which satisfies  $\sum_{j=1}^X \mathcal{P}_j = 1$  and the Rényi entropy is defined as

$$\mathcal{S}_{RE} = \frac{1}{\zeta} \ln \sum_{j=1}^X \mathcal{P}_j^{1-\zeta}. \quad (19)$$

Here,  $\zeta = 1 - \mathcal{N}$  ( $\mathcal{N}$  is the free parameter). Boltzmann-Gibbs entropy is recovered by substituting  $\mathcal{N} = 1$  in the above two equations. The Rényi entropy in terms of black hole entropy is defined as

$$\mathcal{S}_{RE} = \frac{1}{\zeta} \ln(1 + \zeta \mathcal{S}_{BH}), \quad (20)$$

Using the thermodynamic relation  $\rho dV \propto T d\mathcal{S}$ , where  $T = \frac{1}{2\pi\mathcal{L}}$  represents the Cai-Kim temperature associated with a system characterized by the IR cutoff  $\mathcal{L}$  and  $\mathcal{S}$  denotes the horizon entropy, we derive the energy density for the RHDE model as

$$\rho_{RDE} = \frac{3\mathcal{C}^2}{8\mathcal{L}^2\pi(1 + \zeta\mathcal{L}^2)}. \quad (21)$$

Here,  $\mathcal{C}$  signifies a dimensionless quantity. For the Hubble horizon this equation turns out to be

$$\rho_{RDE} = \frac{3\mathcal{C}^2 H^2}{8\mathcal{L}^2\pi(1 + \frac{\zeta}{H^2})}. \quad (22)$$

By specifically adopting the Hubble radius as the IR cutoff, this formulation gives a direct connection between the thermodynamic properties of the horizon and the evolution of DE.

We assume that the power-law scale factor naturally arises as a solution to the Friedmann equations under specific assumptions about the dominant energy component and is given as

$$\mathbf{a}(t) = \mathbf{a}_o \left( \frac{t}{t_o} \right)^\delta e^{\eta \left( \frac{t}{t_o} - 1 \right)}. \quad (23)$$

Here,  $\delta$  and  $\eta$  are non-zero positive constants and  $t_o$  determines the cosmic age, while the relationship between time and redshift follows the Lambert function distribution as  $t(z) = \frac{st_o}{l} g(z)$ , where  $s$  and  $l$  are positive constants. The parameters appearing in Eq.(23) are carefully selected to capture the essential features of cosmic evolution in a viable observational framework. The constant  $\mathbf{a}_o$  serves as a normalization factor, ensuring that the scale factor is dimensionally consistent and provides a convenient initial reference for the expansion history. The parameter  $\delta$  governs the power-law contribution to the scale factor, thereby controlling the early-time expansion dynamics and influencing the rate of transition toward accelerated phases. The exponential contribution determined by  $\eta$  plays a central role in generating late-time acceleration, mimicking the effect of DE-like components. Furthermore, the parameter  $t_o$  denotes a characteristic time scale against which cosmic evolution is measured, allowing the model to maintain consistency with cosmological timescales inferred from observations. The adopted parameter values are chosen to ensure a positive and monotonically increasing scale factor and Hubble parameter, consistent with the scenario of cosmic

accelerated expansion. This expression can be rewritten as

$$g(z) = \text{Lambert}W\left(\frac{l}{s}e^{\frac{l-\ln(1+z)}{s}}\right). \quad (24)$$

The Hubble parameter turns out to be

$$H = \frac{\delta}{t} + \frac{\eta}{t_o}. \quad (25)$$

Cosmic chronometers (CC) provide a significant tool to determine the Hubble expansion rate by analyzing the relative ages of galaxies. This approach relies on passively evolving galaxies, which are galaxies that have stopped forming new stars and are mainly composed of old stellar populations. By analyzing the ages and metallicities of such galaxies at different redshifts, one can determine how fast the cosmos is expanding. The basic idea is that the Hubble parameter  $H_{CC}(z) = \frac{1}{1+z_{CC}} \frac{dz_{CC}}{dt}$ , can be estimated from the rate of change of redshift with respect to cosmic time. In other words, by comparing the ages of galaxies at slightly different redshifts, we can infer how the redshift changes over time, and thus obtain the expansion rate at that redshift [62]. In this study, we use cosmic chronometer data compiled from several observational sources, covering the redshift range  $0.07 \leq z \leq 1.97$  [63]. This dataset provides valuable, model-independent information for constraining cosmological models and studying the universe expansion history. Figure 1 shows the evolution of Hubble parameter against the redshift variable. The blue colour represents the CC dataset and its error bars. The figure determines that the our model is aligned with  $\Lambda$ CDM model at lower redshifts. This alinement refers that the choice of parameters significantly explains the current cosmic expansion.

The deceleration parameter ( $q$ ) quantifies the rate of change in the universe expansion and is defined as

$$q = -1 - \dot{H}H^{-2}. \quad (26)$$

Its value distinguishes between accelerating ( $q < 0$ ) and decelerating ( $q > 0$ ) cosmic expansion, making it crucial for understanding the impact of different energy components. From Eqs.(25) and (26), we obtain

$$q = -1 + \frac{t_o^2 \delta}{(t_o \delta + \eta t)^2}. \quad (27)$$

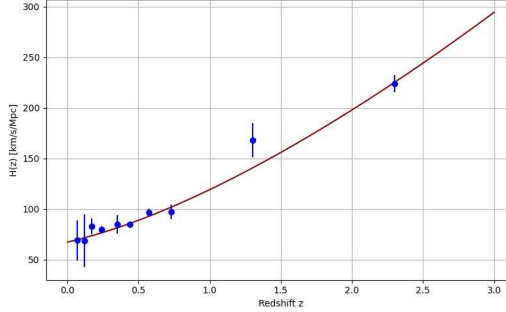


Figure 1: Trajectory of the Hubble Parameter against  $z$  using CC dataset.

Figure 2 presents the graphical behavior of the scale factor, Hubble parameter and deceleration parameter as functions of the redshift variable. The analysis is conducted for the parameter values  $\mathbf{a}_o = 10$ ,  $l = 15$ ,  $\delta = 10$ ,  $\eta = 1.5$  and  $t_o = 20$ . The results indicate that both the scale factor and the Hubble parameter remain positive, signifying an accelerated cosmic expansion. This acceleration is further supported by the negative behavior of the deceleration parameter, providing additional confirmation of the cosmic late time accelerated dynamics.

The Ricci scalar for the flat FRW universe is obtained by using Eq.(25) as

$$R = 6\dot{H} + 2H^2 = \frac{6(t_o^2\delta(2\delta - 1) + 4\delta\eta t_o t + 2\eta^2 t^2)}{t_o^2 t^2}. \quad (28)$$

Inserting Eq.(25) into (22), we obtain

$$\rho_{RDE} = \frac{3\mathcal{C}^2(t_o\delta + \eta t)^4}{8\pi t_o^2 t^2 (\delta^2 + \pi\zeta t^2) + 2\delta\eta t_o t + \eta^2 t^2}. \quad (29)$$

Using Eqs.(25), (28) and (29) into (14) and (15), the energy density and pressure for DE turn out to be

$$\begin{aligned} \rho_{DE} &= \frac{2^{-n-6}3^{1-n}}{\alpha n} \left[ \frac{2\eta^2}{t_o^2} + \frac{4\delta\eta}{t_o t} + \frac{\delta(2\delta - 1)}{t^2} \right]^{1-n} \left[ \alpha 2^{n+6} \left( \frac{6\eta^2}{t_o^2} + \frac{12\delta\eta}{t_o t} \right. \right. \\ &+ \left. \left. \frac{3\delta(2\delta - 1)}{t^2} \right)^n - 2^{n+6} n \alpha \left( \frac{6\eta^2}{t_o^2} + \frac{12\delta\eta}{t_o t} + \frac{3\delta(2\delta - 1)}{t^2} \right)^n \right] \end{aligned}$$

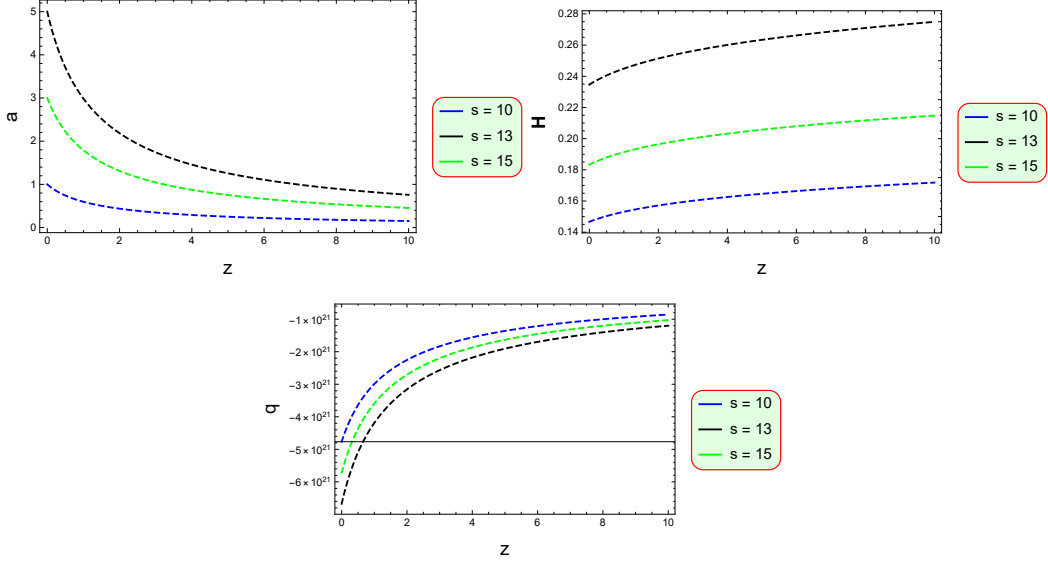


Figure 2: Parametric evolution of scale factor, Hubble Parameter and deceleration parameter.

$$\begin{aligned}
& + \frac{9\beta\mathcal{C}^4(t_o\delta + \eta t)^8}{\pi^2 t_o^4 t^4 \left( \pi\alpha t_o^2 t^2 + (t\delta + \eta t)^2 \right)^2} + \left( 2^{n+7} n\alpha(n-1) t_o^2 \delta (t_o\delta + \eta t)^8 \right. \\
& + \eta t) (t_o(2\delta - 1) + 2\eta t) \left( \frac{6\eta^2}{t_o^2} + \frac{12\delta\eta}{t_o t} + \frac{3\delta(2\delta - 1)}{t^2} \right)^n \Big) \\
& \times \left( t_o^2 \delta (2\delta - 1) + 4t_o \delta \eta t + 2\eta^2 t^2 \right)^{-2} + \left( 6\mathcal{C}^2 (t_o\delta + \eta t)^4 \left( \pi\alpha t_o^2 \delta^2 + \pi\alpha t_o^2 t^2 \right) \right. \\
& - 2^{n+2} n t^2 \left( \frac{6\eta^2}{b^2} + \frac{12\delta\eta}{t_o t} + \frac{3\delta(2\delta - 1)}{t^2} \right)^{n-1} \left( t_o^2 \left( \delta^2 + \pi\alpha t_o^2 t^2 \right) \right. \\
& + 2t_o \delta \eta t + \eta^2 t^2 \Big) + 8\pi t_o^2 t^2 \left( \pi\alpha t_o^2 t^2 + (t_o\delta + \eta t)^2 \right) \\
& \left. \left. + 3\beta\mathcal{C}^2 (t_o\delta + \eta t)^4 \right) \right) \left( \pi^2 t_o^4 t^4 \left( \pi\alpha t_o^2 t^2 + (b\delta + \eta t)^2 \right)^2 \right)^{-1} \Big], \quad (30)
\end{aligned}$$

$$p_{RDE} = \frac{6^{-n}}{\alpha n} \left[ \frac{2\eta^2}{t_o^2} + \frac{4\delta\eta}{t_o t} + \frac{\delta(2\delta - 1)}{t^2} \right]^{1-n} \left[ - \left( 144\alpha\delta n(n-1)(t_o\delta + \eta t)^8 \right) \right]$$

$$\begin{aligned}
& + \eta t) (t_o (2\delta - 1) + 2\eta t) \Big) \left( t_o^2 t^4 \right)^{-1} \alpha + 3^{n+1} \left( \frac{4\eta^2}{t_o^2} + \frac{8\delta\eta}{bt} \right. \\
& + \frac{2\delta(2\delta - 1)}{t^2} \Big)^n \alpha - 3^{n+1} n \left( \frac{4\eta^2}{t_o^2} + \frac{8\delta\eta}{t_o t} + \frac{2\delta(2\delta - 1)}{t^2} \right)^n \\
& - \frac{27\beta\mathcal{C}^4(t_o\delta + \eta t)^8}{64\pi^2 t_o^4 t^4 \left( \pi\alpha t_o^2 t^2 + (t_o\delta + \eta t)^2 \right)^2} + \left( \alpha t_o^4 \delta^2 2^{n+2} n (n \right. \\
& - 1) (n - 2) (-2t_o\delta + t_o - 2\eta t)^2 \left( \frac{6\eta^2}{t_o^2} + \frac{12\delta\eta}{t_o t} + (3\delta(2\delta \right. \\
& - 1)) (t^2)^{-1} \Big)^n \Big) \left( \left( t_o^2 \delta (2\delta - 1) + 4t_o \delta \eta t + 2\eta^2 t^2 \right)^3 \right)^{-1} + \\
& \left. \left( \alpha t_o^3 \delta 2^{n+1} n (n - 1) (t_o (6\delta - 3) + 4\eta t) \left( \frac{6\eta^2}{t_o^2} + \frac{12\delta\eta}{t_o t} + \right. \right. \right. \\
& \left. \left. \left. \frac{3\delta(2\delta - 1)}{t^2} \right)^n \right) \left( t_o^2 \delta (2\delta - 1) + 4t_o \delta \eta t + 2\eta^2 t^2 \right)^{-2} \right]. \quad (31)
\end{aligned}$$

The equation of state (EoS) parameter, defined as  $\omega = \frac{p}{\rho}$ , determines the relationship between the matter variables in a given cosmological framework. In the background of EMSG, this parameter is significant for exploring the dynamic history of the cosmos. The condition where  $\omega < -1$  characterizes the phantom era, in this epoch the energy density increases with the cosmic expansion. The quintessence phase is determined when as  $\omega \in (-1, -\frac{1}{3})$ , indicating a type of DE that facilitates accelerated growth. The interplay between these epochs, is governed by the intrinsic dynamics of the  $f(R, T^2)$  model. In this framework, the EoS parameter associated with RHDE is determined through the expression  $\omega_{RDE} = \frac{p_{RDE}}{\rho_{RDE}}$  as

$$\begin{aligned}
\omega_{RDE} & = \frac{64}{3} \left[ -\frac{144\alpha\delta n(n-1)(t_o\delta + \eta t)(t_o(2\delta - 1) + 2\eta t)}{t_o^2 t^4} \right. \\
& + \alpha 3^{n+1} \left( \frac{4\eta^2}{t_o^2} + \frac{8\delta\eta}{t_o t} + \frac{2\delta(2\delta - 1)}{t^2} \right)^n - 3^{n+1} \alpha n \left( \frac{4\eta^2}{t_o^2} \right. \\
& + \frac{8\delta\eta}{t_o t} + \frac{2\delta(2\delta - 1)}{t^2} \Big)^n - \frac{27\beta\mathcal{C}^4(t_o\delta + \eta t)^8}{64\pi^2 t_o^4 t^4 \left( \pi\alpha t_o^2 t^2 + (t_o\delta + \eta t)^2 \right)^2} \\
& \left. + \left( \alpha t_o^4 \delta^2 2^{n+2} n (n - 1) (n - 2) (-2t_o\delta + t_o - 2\eta t)^2 \left( \frac{6\eta^2}{t_o^2} \right. \right. \right. \\
& \left. \left. \left. \right)^{-1} \right) \left( \left( t_o^2 \delta (2\delta - 1) + 4t_o \delta \eta t + 2\eta^2 t^2 \right)^3 \right)^{-1} + \\
& \left. \left. \left( \alpha t_o^3 \delta 2^{n+1} n (n - 1) (t_o (6\delta - 3) + 4\eta t) \left( \frac{6\eta^2}{t_o^2} + \frac{12\delta\eta}{t_o t} + \right. \right. \right. \\
& \left. \left. \left. \frac{3\delta(2\delta - 1)}{t^2} \right)^n \right) \left( t_o^2 \delta (2\delta - 1) + 4t_o \delta \eta t + 2\eta^2 t^2 \right)^{-2} \right].
\end{aligned}$$

$$\begin{aligned}
& + \left( \frac{12\delta\eta}{t_o t} + \frac{3\delta(2\delta-1)}{t^2} \right)^n \left( \left( t_o^2 \delta(2\delta-1) + 4t_o \delta \eta t + 2\eta^2 \right. \right. \\
& \times \left. t^2 \right)^3 \left. \right)^{-1} + \left( \alpha t_o^3 \delta 2^{n+1} n(n-1) (t_o(6\delta-3) + 4\eta t) \left( \frac{6\eta^2}{t_o^2} \right. \right. \\
& + \left. \frac{12\delta\eta}{t_o t} + \frac{3\delta(2\delta-1)}{t^2} \right)^n \left( t_o^2 \delta(2\delta-1) + 4t_o \delta \eta t + 2\eta^2 t^2 \right)^{-2} \left. \right] \\
& \left[ \alpha 2^{n+6} (1-n) \left( \frac{6\eta^2}{t_o^2} + \frac{12\delta\eta}{t_o t} + \frac{3\delta(2\delta-1)}{t^2} \right)^n + \left( 9\beta \mathcal{C}^4 \right. \right. \\
& \times \left. (t_o \delta + \eta t)^8 \right) \left( \pi^2 t_o^4 t^4 \left( \pi \alpha t_o^2 t^2 + (t_o \delta + \eta t)^2 \right)^2 \right)^{-1} + \left( \alpha t_o^2 \right. \\
& \times \left. \delta 2^{n+7} n(n-1) (t_o \delta + \eta t) (t_o(2\delta-1) + 2\eta t) \left( \frac{6\eta^2}{t_o^2} + \frac{12\delta\eta}{t_o t} \right. \right. \\
& + \left. \frac{3\delta(2\delta-1)}{t^2} \right)^n \left( \left( t_o^2 \delta(2\delta-1) + 4t_o \delta \eta t + 2\eta^2 t^2 \right)^2 \right)^{-1} \\
& + \left( 6\mathcal{C}^2 (t_o \delta + \eta t)^4 \left( \pi \alpha t_o^2 - 2^{n+2} n t^2 \left( \frac{6\eta^2}{t_o^2} + \frac{12\delta\eta}{t_o t} \right. \right. \right. \\
& + \left. \frac{3\delta(2\delta-1)}{t^2} \right)^{n-1} \left( t_o^2 \left( \delta^2 + \pi \alpha t^2 \right) + 2t_o \delta \eta t + \eta^2 t^2 \right) \\
& + \left. \left. 8\pi t_o^2 t^2 \left( \pi \alpha t_o^2 t^2 + (t_o \delta + \eta t)^2 \right) + 3\beta \mathcal{C}^2 (t_o \delta + \eta t)^4 \right) \right) \\
& \times \left. \left( \pi^2 t_o^4 t^4 \left( \pi \alpha t_o^2 t^2 + (t_o \delta + \eta t)^2 \right)^2 \right)^{-1} \right]^{-1}. \tag{32}
\end{aligned}$$

Figure 3 illustrates the behavior of the energy density for RHDE, which remains positive and increases over time as the cosmos evolved into the future. The behavior of the matter variables associated with DE further supports the scenario of accelerated cosmic expansion. Moreover, the EoS parameter exhibits the phantom regime, indicating an accelerated cosmic expansion.

## Stability Analysis

The stability analysis of a cosmological model is vital for determining its physical viability and consistency with observational data. In the context of

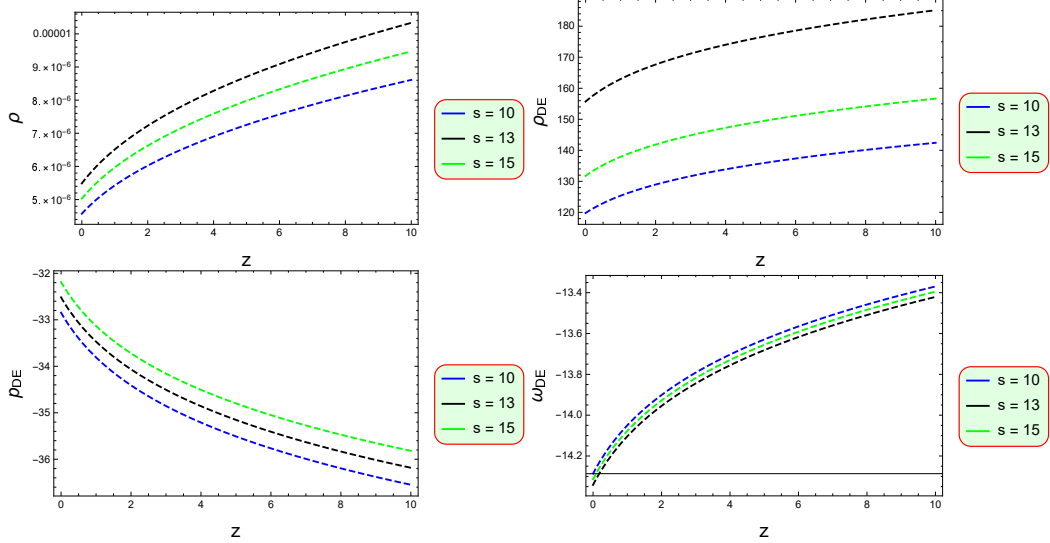


Figure 3: Graphical analysis of  $\rho$ ,  $\rho_{DE}$ ,  $p_{DE}$  and  $\omega_{DE}$  for different parametric values.

the RHDE model, evaluating stability provides insights into the long-term behavior of cosmic evolution. To examine the stability of the model against perturbations, we employ the squared sound speed parameter, which is a key diagnostic tool for determining whether perturbations in the DE component grows or dissipates over time. A positive squared sound speed indicates stability, while a negative value suggests an instability in the fluctuation regime. This parameter is given as

$$\nu_s^2 = \frac{\dot{P}_{DE}}{\dot{\rho}_{DE}}. \quad (33)$$

By substituting Eqs.(30) and (31) into the above equation, we obtain the squared sound speed parameter, whose behavior is illustrated in Figure 3, demonstrating that it remains positive. This indicates that the RHDE model exhibits stability against small perturbations, ensuring that fluctuations in the DE component do not grow over time. Consequently, the positive squared sound speed supports the physical viability of the model in describing the accelerated expansion of the universe.

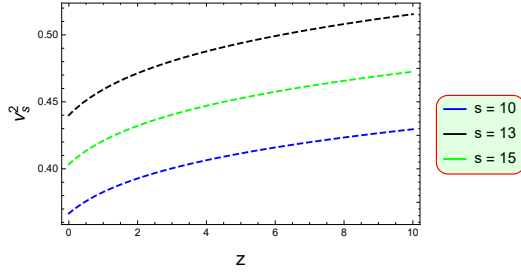


Figure 4: Trajectories of squared sound speed parameter for considered parametric values.

### 3.2 Sharma-Mittal Holographic Dark Energy Model

Sharma-Mittal entropy generalizes both Renyi and Tsallis entropies, addressing the limitations of classical Shannon entropy in complex systems with long range interactions and non-extensive behavior. By incorporating two parameters, one controlling scaling from RE and the other deformation from TE it provides great flexibility in modeling diverse physical, statistical and cosmological systems. This unification allows for a more comprehensive measure of uncertainty, making it valuable in non-equilibrium dynamics, power law distributions and multifractal structures. This entropy is given as

$$\mathcal{S}_{SMDE} = \frac{1}{1-\tau} \left[ \left( \sum_{j=1}^X \mathcal{P}_j^{1-\zeta} \right)^{\frac{1-\tau}{\zeta}} - 1 \right]. \quad (34)$$

Here, the free parameter  $\tau = 1 - \mathcal{B}$ . This equation takes the form

$$\mathcal{S}_{SMDE} = \frac{1}{\mathcal{B}} \left[ \left( 1 + \frac{\chi \mathcal{A}}{4} \right)^{\frac{\mathcal{B}}{\chi}} - 1 \right], \quad (35)$$

where we use parametric generalized entropies  $\mathcal{S} = \frac{1}{\zeta} \ln \sum_{j=1}^X \mathcal{P}_j^{1-\zeta}$ ,  $\mathcal{S}_T = \frac{1}{6} \sum_{j=1}^X \left( \mathcal{P}_j^{1-\zeta} - \mathcal{P}_j \right)$  and the relation  $\mathcal{S}_T = \frac{\mathcal{A}}{4}$  with  $\mathcal{A}$  represents the horizon area.

In the framework of the holographic principle, the system horizon is intrinsically connected to both the IR and ultraviolet (UV) cutoffs. The UV cutoff, associated with the vacuum energy density, plays a central role in the HDE scenario. In particular, the energy density of DE can be written as

$$\rho_{DE} = \Lambda^4$$

where  $\Lambda$  denotes the UV cutoff. Cohen et al [64] argued that since the maximum energy density in the effective theory is  $\Lambda^4$ , the constraint on  $L$  is  $L^3\Lambda^4 \leq LM_p^2$ , which means that the total energy in a region of size  $L$  must not exceed the mass of a black hole of the same size. This condition enforces a connection between the UV and IR cutoffs, ensuring that effective field theory remains valid within holographic bounds. Although Cohen et al [64] did not explicitly propose the HDE density, their UV-IR relation was later adapted in cosmological contexts, leading to the well known expression for HDE in terms of the IR cutoff, which represents the largest relevant length scale of the system. Consequently, the expression for the holographic energy density is obtained by enforcing these physical constraints, ensuring consistency with the holographic principle as

$$\rho_{SMDE} = \frac{3\mathcal{C}^2}{\mathcal{L}^4\mathcal{B}} \left[ \left( 1 + \chi\pi\mathcal{L}^2 \right)^{\frac{\mathcal{B}}{\chi}} - 1 \right]. \quad (36)$$

This expression for the Hubble horizon turns out to be

$$\rho_{SMDE} = \frac{3\mathcal{C}^2 H^4}{\mathcal{B}} \left[ \left( 1 + \frac{\chi\pi}{H^2} \right)^{\frac{\mathcal{B}}{\chi}} - 1 \right]. \quad (37)$$

Using Eqs.(25), (28) and (37) into Eqs.(14) and (15), the expression for matter variables for DE turn out to be

$$\begin{aligned} \rho_{DE} &= \frac{2^{-n}3^{1-n}}{\alpha n} \left( \frac{2\eta^2}{t_o^2} + \frac{4\delta\eta}{t_o t} + \frac{\delta(2\delta-1)}{t^2} \right)^{1-n} \\ &\times \left[ \alpha 6^n (1-n) \left( \frac{2\eta^2}{t_o^2} + \frac{4\delta\eta}{t_o t} + \frac{\delta(2\delta-1)}{t^2} \right)^n \right. \\ &+ \left. \frac{\beta \left( t_o^4 \mathcal{B} t^4 - 3\mathcal{C}^2 (t_o \delta + \eta t)^4 \left( \frac{\pi t_o^2 t^2 \chi}{(t_o \delta + \eta t)^2} + 1 \right)^{B\chi} \right)^2}{t_o^8 \mathcal{B}^2 t^8} \right. \\ &+ \left. \left( \alpha t_o^2 \delta 2^{n+1} n (n-1) (t_o \delta + \eta t) (t_o (2\delta-1) + 2\eta t) \right. \right. \\ &\times \left. \left. \left( \frac{6\eta^2}{t_o^2} + \frac{12\delta\eta}{t_o t} + \frac{3\delta(2\delta-1)}{t^2} \right)^n \right) \left( \left( t_o^2 \delta (2\delta-1) \right. \right. \right. \\ &+ \left. \left. \left. 4t_o \delta \eta t + 2\eta^2 t^2 \right)^2 \right)^{-1} - \frac{2}{t_o^8 \mathcal{B}^2 t^8} \left( t_o^4 \mathcal{B} t^4 - 3\mathcal{C}^2 (t_o \delta + \eta t)^4 \left( \frac{\pi t_o^2 t^2 \chi}{(t_o \delta + \eta t)^2} + 1 \right)^{B\chi} \right) \right] \end{aligned}$$

$$\begin{aligned}
& \times \delta + \eta t)^4 \left( \frac{\pi t_o^2 t^2 \chi}{(t_o \delta + \eta t)^2} + 1 \right)^{\mathcal{B}\chi} \left( -t_o^4 \beta \mathcal{B} t^4 + t_o^4 \right. \\
& \times \mathcal{B} t^4 + 3\beta \mathcal{C}^2 (t_o \delta + \eta t)^4 \left( \frac{\pi t_o^2 t^2 \chi}{(t_o \delta + \eta t)^2} + 1 \right)^{\mathcal{B}\chi} \\
& + \left. \alpha t_o^4 \mathcal{B} - 6^{n-1} n t^4 \left( \frac{2\eta^2}{t_o^2} + \frac{4\delta\eta}{t_o t} + \frac{\delta(2\delta-1)}{t^2} \right)^{n-1} \right) \Big], \quad (38) \\
p_{DE} &= \frac{6^{-n}}{\alpha n} \left( \frac{2\eta^2}{t_o^2} + \frac{4\delta\eta}{t_o t} + \frac{\delta(2\delta-1)}{t^2} \right)^{1-n} \\
& \times \left[ -\frac{144\alpha\delta n(n-1)(t_o \delta + \eta t)(t_o(2\delta-1) + 2\eta t)}{t_o^2 t^4} \right. \\
& + \left( \alpha t_o^4 \delta^2 2^{n+2} n(n-1)(n-2)(t_o(2\delta-1) + 2\eta t)^2 \right. \\
& \times \left. \left( \frac{6\eta^2}{t_o^2} + \frac{12\delta\eta}{t_o t} + \frac{3\delta(2\delta-1)}{t^2} \right)^n \right) \left( \left( t_o^2 \delta(2\delta-1) \right. \right. \\
& + \left. \left. 4t_o \delta \eta t + 2\eta^2 t^2 \right)^3 \right)^{-1} + \left( \alpha t_o^3 \delta 2^{n+1} n(n-1)(t_o \right. \\
& \times (6\delta-3) + 4\eta t) \left( \frac{6\eta^2}{t_o^2} + \frac{12\delta\eta}{t_o t} + \frac{3\delta(2\delta-1)}{t^2} \right)^n \Big) \\
& \times \left( \left( t_o^2 \delta(2\delta-1) + 4t_o \delta \eta t + 2\eta^2 t^2 \right)^2 \right)^{-1} + \left( 3 \right. \\
& \times \left. \left( \alpha t_o^8 \mathcal{B}^2 6^n t^8 \left( \frac{2\eta^2}{t_o^2} + \frac{4\delta\eta}{t_o t} + \frac{\delta(2\delta-1)}{t^2} \right)^n - \alpha t_o^8 \right. \right. \\
& \times \left. \left. \mathcal{B}^2 6^n n t^8 \left( \frac{2\eta^2}{t_o^2} + \frac{4\delta\eta}{t_o t} + \frac{\delta(2\delta-1)}{t^2} \right)^n \right. \right. \\
& - \left. \beta \left( t_o^4 \mathcal{B} t^4 - 3\mathcal{C}^2 (t_o \delta + \eta t)^4 \left( \frac{\pi t_o^2 t^2 \chi}{(t_o \delta + \eta t)^2} \right. \right. \right. \\
& \left. \left. \left. + 1 \right)^{\mathcal{B}\chi} \right)^2 \right) \left( t_o^8 \mathcal{B}^2 t^8 \right)^{-1} \Big]. \quad (39)
\end{aligned}$$

The corresponding EoS parameter for the SMHDE is given as

$$\omega_{DE} = \left[ -\frac{144\alpha\delta n(n-1)(t_o \delta + \eta t)(t_o(2\delta-1) + 2\eta t)}{t_o^2 t^4} \right.$$

$$\begin{aligned}
& + \left( \alpha t_o^4 \delta^2 2^{n+2} n(n-)(n-2)(t_o(2\delta-1) + 2\eta t)^2 \left( \frac{6\eta^2}{t_o^2} \right. \right. \\
& + \left. \left. \frac{12\delta\eta}{t_o t} + \frac{3\delta(2\delta-1)}{t^2} \right)^n \right) \left( \left( t_o^2 \delta(2\delta-1) + 4t_o \delta \eta t + \right. \right. \\
& \left. \left. 2\eta^2 t^2 \right)^3 \right)^{-1} + \left( \alpha t_o^3 \delta 2^{n+1} n(n-1)(t_o(6\delta-3) + 4\eta t) \right. \\
& \times \left. \left( \frac{6\eta^2}{t_o^2} + \frac{12\delta\eta}{t_o t} + \frac{3\delta(2\delta-1)}{t^2} \right)^n \right) \left( \left( t_o^2 \delta(2\delta-1) + 4t_o \right. \right. \\
& \times \left. \left. \delta \eta t + 2\eta^2 t^2 \right)^2 \right)^{-1} + \frac{3}{t_o^8 \mathcal{B}^2 t^8} \left( \alpha t_o^8 \mathcal{B}^2 6^n t^8 \left( \frac{2\eta^2}{t_o^2} + \frac{4\delta\eta}{t_o t} \right. \right. \\
& + \left. \left. \frac{\delta(2\delta-1)}{t^2} \right)^n - \alpha t_o^8 \mathcal{B}^2 6^n n t^8 \left( \frac{2\eta^2}{t_o^2} + \frac{4\delta\eta}{t_o t} + \frac{\delta(2\delta-1)}{t^2} \right)^n \right. \\
& - \left. \beta \left( t_o^4 \mathcal{B} t^4 - 3\mathcal{C}^2 (t_o \delta + \eta t)^4 \left( \frac{\pi t_o^2 t^2 \chi}{(t_o \delta + \eta t)^2} + 1 \right)^{\mathcal{B}\chi} \right)^2 \right)^{-1} \Big] \\
& \times \left[ 3 \left( 6^n \alpha (1-n) \left( \frac{2\eta^2}{t_o^2} + \frac{4\delta\eta}{t_o t} + \frac{\delta(2\delta-1)}{t^2} \right)^n + \left( \alpha t_o^2 \delta \right. \right. \right. \\
& \times \left. \left. \left. 2^{n+1} n(n-1)(t_o \delta + \eta t)(t_o(2\delta-1) + 2\eta t) \left( \frac{6\eta^2}{t_o^2} + \frac{12\delta\eta}{t_o t} \right. \right. \right. \\
& + \left. \left. \left. \frac{3\delta(2\delta-1)}{t^2} \right)^n \right) \left( \left( t_o^2 \delta(2\delta-1) + 4t_o \delta \eta t + 2\eta^2 t^2 \right)^2 \right)^{-1} \right. \\
& + \left. \left. \beta \left( t_o^4 \mathcal{B} t^4 - 3\mathcal{C}^2 (t_o \delta + \eta t)^4 \left( \frac{\pi t_o^2 t^2 \chi}{(t_o \delta + \eta t)^2} + 1 \right)^{\mathcal{B}\chi} \right)^2 \right. \\
& + \left. \left. \frac{2}{t_o^8 \mathcal{B}^2 t^8} \left( t_o^4 \mathcal{B} t^4 - 3\mathcal{C}^2 (t_o \delta + \eta t)^4 \left( \frac{\pi t_o^2 t^2 \chi}{(t_o \delta + \eta t)^2} \right. \right. \right. \\
& + \left. \left. \left. 1 \right)^{\mathcal{B}\chi} \right) \left( -t_o^4 \beta \mathcal{B} t^4 + t_o^4 \mathcal{B} t^4 + 3\beta \mathcal{C}^2 (t_o \delta + \eta t)^4 \right. \right. \\
& \times \left. \left. \left( \frac{\pi t_o^2 t^2 \chi}{(t_o \delta + \eta t)^2} + 1 \right)^{\mathcal{B}\chi} - \alpha t_o^4 \mathcal{B} 6^{n-1} n t^4 \left( \frac{2\eta^2}{t_o^2} \right. \right. \\
& + \left. \left. \left. \frac{4\delta\eta}{t_o t} + \frac{\delta(2\delta-1)}{t^2} \right)^{n-1} \right) \right) \right]^{-1}. \tag{40}
\end{aligned}$$

Figure 5 demonstrates that the energy density of the SMHDE model

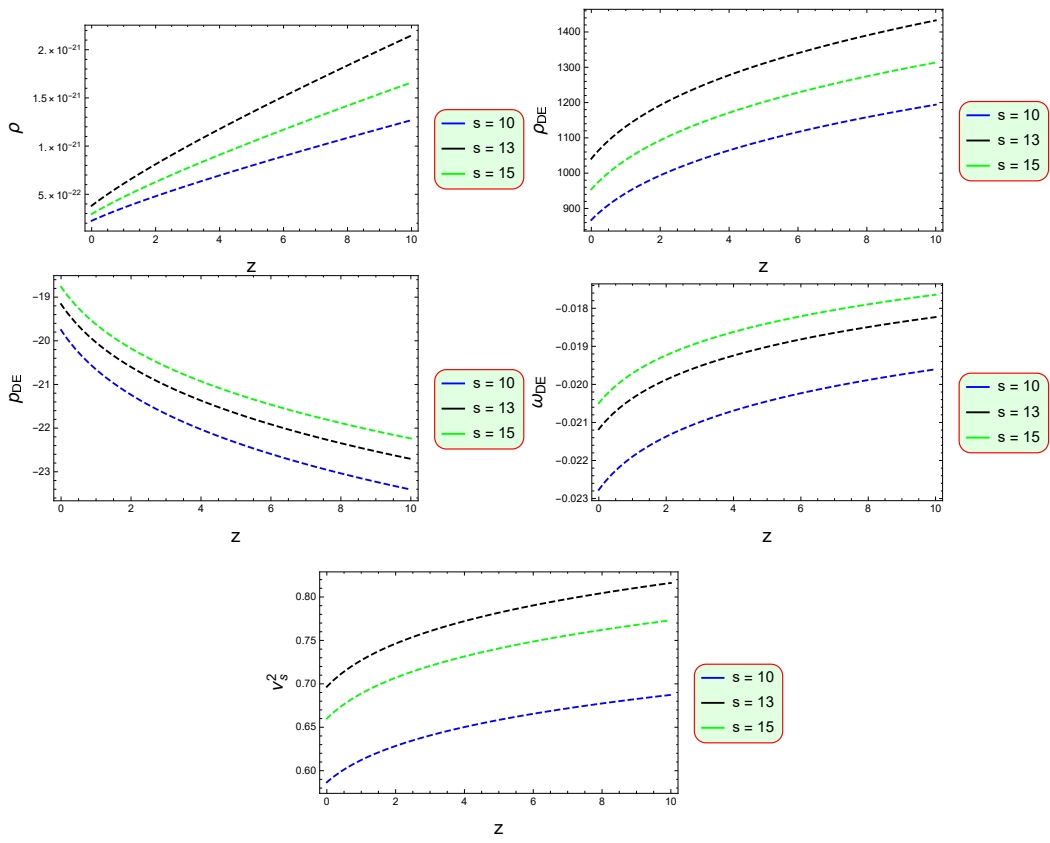


Figure 5: Graphical analysis of  $\rho$ ,  $\rho_{DE}$ ,  $p_{DE}$ ,  $\omega_{DE}$  and  $\nu_s^2$ .

remains positive and increases in the late-time evolution of the universe. The behavior of energy density and pressure in this DE model indicates an accelerating cosmic expansion, as the energy density remains positive while the pressure takes negative values. Additionally, the EoS parameter falls within the quintessence regime, reinforcing the model role in driving the accelerated expansion of the universe. Furthermore, the stability analysis, conducted through the squared sound speed parameter, confirms that the model remains dynamically stable throughout its evolution.

### 3.3 Generalized Holographic Dark Energy Model

The GHDE extends the standard HDE framework to address the fine-tuning and coincidence problem associated with the cosmological constant. By incorporating modified IR cutoffs interactions with dark matter or higher-order curvature corrections, GHDE provides a more flexible description of DE dynamics. This generalization allows for better consistency with observational constraints and also aligning with modified gravity theories. Thus, the GHDE serves as a viable alternative framework for exploring the nature of DE. A novel entropy function incorporating three parameters has been proposed, capable of generalizing various existing entropy measures, including the standard Boltzmann-Gibbs entropy, RE and TE [64]. This entropy characterized by the free parameters  $\mu$ ,  $\nu$  and  $\gamma$  is defined as

$$\mathcal{S}_{GHDE}[\mu, \nu, \gamma] = \frac{1}{\gamma} \left[ \left( 1 + \frac{\mu}{\nu} \mathcal{S}_{BH} \right)^\nu - 1 \right]. \quad (41)$$

The energy density for GHDE is obtained using black hole energy density relation  $\rho = 24\pi\mathcal{C}^2 G \mathcal{L}^2$ , with Hubble radius  $r_H = \frac{1}{H}$  in generalized entropy as

$$\rho_{GHDE} = \frac{3\mathcal{C}^2 H^2}{8\pi\mathcal{B}} \left[ \left( \frac{b\pi}{aH^2} + 1 \right)^a - 1 \right], \quad (42)$$

where  $a$  and  $b$  are non-negative parameters. The energy density and pressure for this DE model are obtained using this equation and Eq.(28) into Eqs.(14) and (15) as

$$\begin{aligned} \rho_{DE} &= \frac{2^{-n-6} 3^{1-n}}{\alpha n} \left( \frac{2\eta^2}{t_o^2} + \frac{4\delta\eta}{t_o t} + \frac{\delta(2\delta-1)}{t^2} \right)^{1-n} \\ &\times \left[ \left( \alpha 2^{n+6} (n-1) \left( \frac{6\eta^2}{t_o^2} + \frac{12\delta\eta}{t_o t} + \frac{3\delta(2\delta-1)}{t^2} \right) \right)^n \right. \end{aligned}$$

$$\begin{aligned}
& \times \left( t_o^4 \delta^2 (2\delta - 1) (-2\delta + 2n + 1) - 2t_o^3 \delta \eta t \left( 8\delta^2 \right. \right. \\
& - 4\delta(n + 1) + n \left. \right) + 4t_o^2 \delta \eta^2 t^2 (-6\delta + n + 1) - \\
& \left. \left. 16t_o \delta \eta^3 t^3 - 4\eta^4 t^4 \right) \right) \left( \left( t_o^2 \delta (2\delta - 1) + 4t_o \delta \eta t \right. \right. \\
& + 2\eta^2 t^2 \left. \right)^2 \left. \right)^{-1} + \frac{27\beta \mathcal{C}^4 (t_o \delta + \eta t)^4}{\pi^2 t_o^4 \mathcal{B}^2 t^4} \left( \left( \frac{\pi a t_o^2 t^2}{b(t_o \delta + \eta t)^2} \right. \right. \\
& + 1 \left. \right)^b - 1 \left. \right)^2 + \frac{8\mathcal{C}^2 (t_o \delta + \eta t)^2}{\pi t_o^2 \mathcal{B} t^2 \left( t_o^2 \delta (2\delta - 1) + 4t_o \delta \eta t + 2\eta^2 t^2 \right)} \\
& \times \left( t_o^2 \left( 6\delta(2\delta - 1) - \alpha 6^n n t^2 \left( \frac{2\eta^2}{t_o^2} + \frac{4\delta\eta}{t_o t} + \frac{\delta(2\delta - 1)}{t^2} \right)^n \right) \right. \\
& + 24t_o \delta \eta t + 12\eta^2 t^2 \left( \left( \frac{\pi a t_o^2 t^2}{b(t_o \delta + \eta t)^2} + 1 \right)^b - 1 \right) \left. \right) \left. \right], \quad (43) \\
p_{DE} & = \frac{6^{-n}}{\alpha n} \left( \frac{2\eta^2}{t_o^2} + \frac{4\delta\eta}{t_o t} + \frac{\delta(2\delta - 1)}{t^2} \right)^{1-n} \left[ -\frac{144\alpha}{b^2 t^4} \delta n \right. \\
& \times (n - 1)(t_o \delta + \eta t)(t_o(2\delta - 1) + 2\eta t) + \left( \alpha t_o^4 \delta^2 2^{n+2} \right. \\
& \times n(n - 1)(n - 2)(t_o(2\delta - 1) + 2\eta t)^2 \left( \frac{6\eta^2}{t_o^2} + \frac{12\delta\eta}{t_o t} \right. \\
& + \left. \frac{3\delta(2\delta - 1)}{t^2} \right)^n \left. \right) \left( \left( t_o^2 \delta (2\delta - 1) + 4t_o \delta \eta t + 2\eta^2 t^2 \right)^3 \right)^{-1} \\
& + \left( \alpha t_o^3 \delta 2^{n+1} n(n - 1)(t_o(6\delta - 3) + 4\eta t) \left( \frac{6\eta^2}{t_o^2} + \frac{12\delta\eta}{t_o t} \right. \right. \\
& + \left. \left. \frac{3\delta(2\delta - 1)}{t^2} \right)^n \right) \left( \left( t_o^2 \delta (2\delta - 1) + 4t_o \delta \eta t + 2\eta^2 t^2 \right)^2 \right)^{-1} \\
& + \left( 3 \left( -9\beta \mathcal{C}^4 (t_o \delta + \eta t)^4 \left( \left( \frac{\pi a t_o^2 t^2}{b(t_o \delta + \eta t)^2} + 1 \right)^b - 1 \right)^2 \right. \right. \\
& + \pi^2 a t_o^4 \mathcal{B}^2 2^{n+6} t^4 \left( \frac{6\eta^2}{t_o^2} + \frac{12\delta\eta}{t_o t} + \frac{3\delta(2\delta - 1)}{t^2} \right)^n \\
& - \left. \left. \pi^2 \alpha t_o^4 \mathcal{B}^2 2^{n+6} n t^4 \left( \frac{6\eta^2}{t_o^2} + \frac{12\delta\eta}{t_o t} + \frac{3\delta(2\delta - 1)}{t^2} \right)^n \right) \right)
\end{aligned}$$

$$\times \left[ \left( 64\pi^2 t_o^4 \mathcal{B}^2 t^4 \right)^{-1} \right]. \quad (44)$$

The EoS parameter for this DE model is expressed as

$$\begin{aligned}
\omega_{DE} = & \frac{64}{3} \left[ -\frac{144\alpha\delta n(n-1)(t_o\delta + \eta t)(t_o(2\delta-1) + 2\eta t)}{t_o^2 t^4} \right. \\
& + \left( \alpha t_o^4 \delta^2 2^{n+2} n(n-1)(n-2)(t_o(2\delta-1) + 2\eta t)^2 \left( \frac{6\eta^2}{t_o^2} \right. \right. \\
& + \left. \left. \frac{12\delta\eta}{t_o t} + \frac{3\delta(2\delta-1)}{t^2} \right)^n \right) \left( \left( t_o^2 \delta(2\delta-1) + 4t_o \delta \eta t + 2\eta^2 \right. \right. \\
& \times \left. \left. t^2 \right)^{-3} + \left( \alpha t_o^3 \delta 2^{n+1} n(n-1)(t_o(6\delta-3) + 4\eta t) \left( \frac{6\eta^2}{t_o^2} \right. \right. \\
& + \left. \left. \frac{12\delta\eta}{t_o t} + \frac{3\delta(2\delta-1)}{t^2} \right)^n \right) \left( t_o^2 \delta(2\delta-1) + 4t_o \delta \eta t + 2\eta^2 t^2 \right)^{-2} \right. \\
& + \left. \left( 3 \left( -9\beta \mathcal{C}^4 (t_o \delta + \eta t)^4 \left( \left( \frac{\pi \alpha t_o^2 t^2}{b(a\delta + \eta t)^2} + 1 \right)^b - 1 \right)^2 + \pi^2 \right. \right. \right. \\
& \times \left. \left. \left. \alpha t_o^4 \mathcal{B}^2 2^{n+6} t^4 \left( \frac{6\eta^2}{t_o^2} + \frac{12\delta\eta}{t_o t} + \frac{3\delta(2\delta-1)}{t^2} \right)^n - \pi^2 \alpha t_o^4 \mathcal{B}^2 2^{n+6} \right. \right. \right. \\
& \times \left. \left. \left. nt^4 \left( \frac{6\eta^2}{t_o^2} + \frac{12\delta\eta}{t_o t} + \frac{3\delta(2\delta-1)}{t^2} \right)^n \right) \right) \left( 64\pi^2 t_o^4 \mathcal{B}^2 t^4 \right)^{-1} \right] \\
& \times \left[ 3 \left( \left( \alpha 2^{n+6} (n-1) \left( \frac{6\eta^2}{t_o^2} + \frac{12\delta\eta}{t_o t} + \frac{3\delta(2\delta-1)}{t^2} \right)^n \left( t_o^4 \delta^2 \right. \right. \right. \right. \\
& \times \left. \left. \left. \left. (2\delta-1)(-2\delta+2n+1) - 2t_o^3 \delta \eta t \left( 8\delta^2 - 4\delta(n+1) + n \right) \right) \right. \right. \right. \\
& + \left. \left. \left. 4t_o^2 \delta \eta^2 t^2 (-6\delta+n+1) - 16t_o \delta \eta^3 t^3 - 4\eta^4 t^4 \right) \right) \left( b^2 \delta(2\delta-1) + 4b\delta \eta t + 2\eta^2 t^2 \right)^{-2} \right) + \left( 8\mathcal{C}^2 (t_o \delta + \eta t)^2 \left( t_o^2 \left( 6\delta(2\delta-1) - \alpha 6^n n t^2 \left( \frac{2\eta^2}{t_o^2} + \frac{4\delta\eta}{t_o t} + \frac{\delta(2\delta-1)}{t^2} \right)^n \right) + 24t_o \delta \eta t + 12\eta^2 t^2 \right) \left( \left( \frac{\pi \alpha t_o^2 t^2}{b(a\delta + \eta t)^2} + 1 \right)^b - 1 \right) \right) \left( \pi t_o^2 \mathcal{B} t^2 \right)
\end{aligned}$$

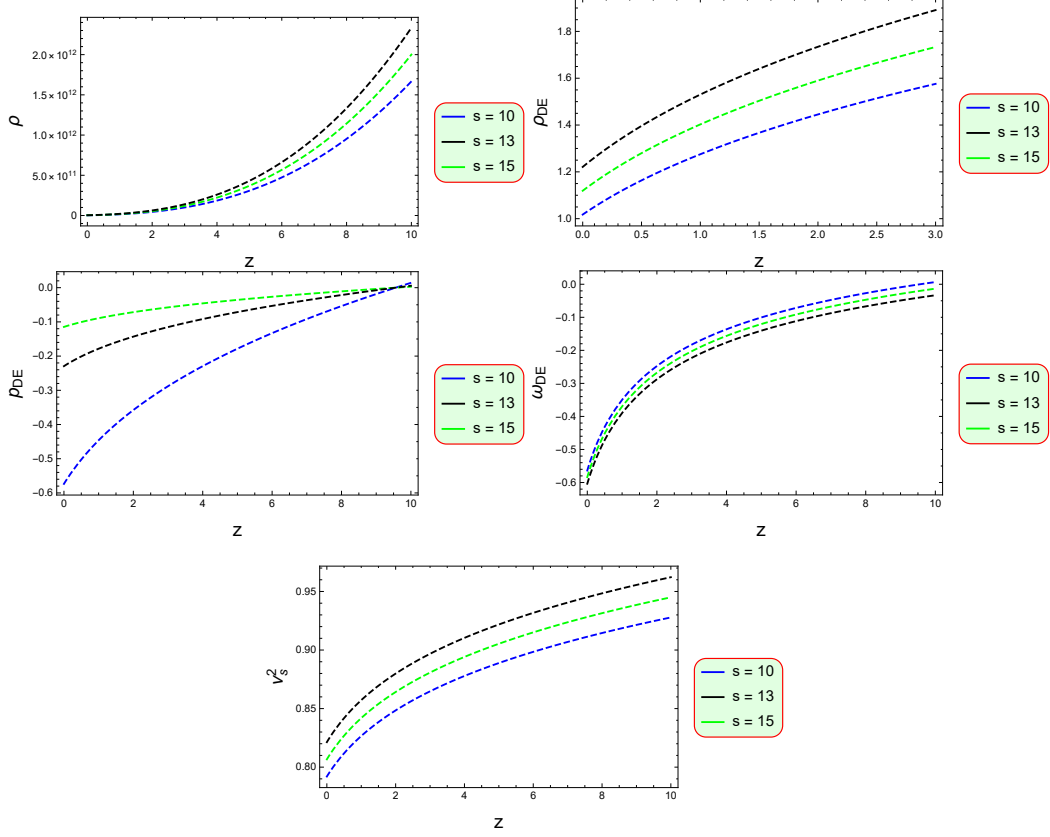


Figure 6: Parametric behavior of  $\rho$ ,  $\rho_{DE}$ ,  $p_{DE}$ ,  $\omega_{DE}$  and  $\nu_s^2$ .

$$\begin{aligned}
& \times \left( t_{\circ}^2 \delta (2\delta - 1) + 4t_{\circ} \delta \eta t + 2\eta^2 t^2 \right) + \frac{27\beta C^4}{\pi^2 t_{\circ}^4 B^2 t^4} (t_{\circ} \\
& \times \delta + \eta t)^4 \left( \left( \frac{\pi \alpha t_{\circ}^2 t^2}{b(a\delta + \eta t)^2} + 1 \right)^b - 1 \right)^2 \Big]^{-1}. \quad (45)
\end{aligned}$$

Figure 6 determines that the energy density of the GHDE model remains positive and increases over time, contributing to the universe accelerated expansion. This behavior is further supported by the matter variables for the DE associated with the model. The EoS parameter transitions from the phantom regime in the early universe to the quintessence regime at late times, highlighting its evolving nature in cosmic dynamics. Additionally, stability analysis using the squared sound speed parameter confirms the model

dynamical consistency throughout its evolution.

## 4 Ricci Horizon

The Ricci horizon  $L_R = \sqrt{H^2 + (\dot{H})^2}$  is introduced as a dynamically motivated length scale that depends on both the Hubble parameter  $H$  and its time derivative  $\dot{H}$ , thereby incorporating the effects of cosmic expansion and its evolution. It is directly related to the Ricci scalar curvature of spacetime, making it a natural geometric quantity for describing the large-scale dynamics of the universe. In holographic DE models, the Ricci horizon serves as a physically consistent infrared cutoff that connects the dark energy density with spacetime curvature. Unlike the event horizon, it is a local quantity and does not rely on the future evolution of the scale factor, thus avoiding causality problems while maintaining compatibility with observational cosmology.

### 4.1 Rényi Holographic Dark Energy Model

The Rényi HDE density corresponding to the Ricci horizon can be formulated by employing Eq. (21) together with the Ricci length scale  $L_R = \sqrt{H^2 + (\dot{H})^2}$  as

$$\rho_{RDE} = \frac{3\mathcal{C}^2(t_o\delta + \eta t)^4}{8\pi t_o^2 t^2 (t_o^2(\delta^2 + \pi\alpha t^2) + 2t_o\delta\eta t + \eta^2 t^2)}. \quad (46)$$

The expression for the matter variables for DE are obtained using Eqs.(25), (28) and (46) into (14) and (15), as

$$\begin{aligned} \rho_{DE} &= \frac{2^{-n-6}3^{1-n}}{\alpha n} \left( \frac{2\eta^2}{t_o^2} + \frac{4\delta\eta}{t_o t} + \frac{\delta(2\delta-1)}{t_o^2 t^2} \right)^{1-n} \\ &\times \left[ \alpha 2^{n+6} \left( \frac{6\eta^2}{t_o^2} + \frac{12\delta\eta}{t_o t} + \frac{3\delta(2\delta-1)}{t^2} \right)^n \right. \\ &- \left. \alpha 2^{n+6} n \left( \frac{6\eta^2}{t_o^2} + \frac{12\delta\eta}{t} + \frac{3\delta(2\delta-1)}{t^2} \right)^n \right. \\ &+ \left. \frac{9\beta\mathcal{C}^4(t_o\delta + \eta t)^8}{\pi^2 t_o^4 t^4 \left( \pi\alpha t_o^2 t^2 + (t_o\delta + \eta t)^2 \right)^2} \right] \end{aligned}$$

$$\begin{aligned}
& + \left( \alpha t_o^2 \delta 2^{n+7} (n-1) n (t_o \delta + \eta t) (t_o (2\delta - 1) + 2\eta t) \right. \\
& \times \left( \frac{6\eta^2}{t_o^2} + \frac{12\delta\eta}{t_o t} + \frac{3\delta(2\delta - 1)}{t^2} \right)^n \\
& \times \left( t_o^2 \delta (2\delta - 1) + 4t_o \delta \eta t + 2\eta^2 t^2 \right)^{-2} \Big) \\
& + \left( 6\mathcal{C}^2 (t_o \delta + \eta t)^4 \left( 3\beta \mathcal{C}^2 (t_o \delta + \eta t)^4 - \pi \alpha t_o^2 2^{n+2} n t^2 \right) \right. \\
& \times \left( \frac{6\eta^2}{t_o^2} + \frac{12\delta\eta}{t_o t} + \frac{3\delta(2\delta - 1)}{t_o^2 t^2} \right)^{n-1} t_o^2 \left( \delta^2 + \pi \alpha t^2 \right) \\
& + \left. 2\delta\eta t_o t + \eta^2 t^2 + 8\pi t_o^2 t^2 (\pi \alpha t_o^2 t^2 + (t_o \delta + \eta t)^2) \right) \\
& \times \left. \left( \pi^2 t_o^4 t^4 (\pi \alpha t_o^2 t^2 + (t_o \delta + \eta t)^2)^2 \right)^{-1} \right]. \tag{47}
\end{aligned}$$

$$\begin{aligned}
p_{DE} & = \frac{6^{-n}}{\alpha n} \left[ \frac{2\eta^2}{t_o^2} + \frac{4\delta\eta}{t_o t} + \frac{\delta(2\delta - 1)}{t^2} \right]^{1-n} \\
& \times \left[ - \frac{144\alpha\delta(n-1)n(t_o \delta + \eta t)(t_o (2\delta - 1) + 2\eta t)}{t_o^2 t^4} \right. \\
& + \alpha 3^{n+1} \left( \frac{4\eta^2}{t_o^2} + \frac{8\delta\eta}{t_o t} + \frac{2\delta(2\delta - 1)}{t^2} \right)^n \\
& - \alpha 3^{n+1} n \left( \frac{4\eta^2}{t_o^2} + \frac{8\delta\eta}{t_o t} + \frac{2\delta(2\delta - 1)}{t^2} \right)^n \\
& + \left( \alpha t_o^4 \delta^2 2^{n+2} (n-2)(n-1)n(-2t_o \delta + t_o - 2\eta t)^2 \right. \\
& \times \left( \frac{6\eta^2}{t_o^2} + \frac{12\delta\eta}{t_o t} + \frac{3\delta(2\delta - 1)}{t^2} \right)^n \left( t_o^2 \delta (2\delta - 1) \right. \\
& + \left. 4\delta\eta t_o t + 2\eta^2 t^2 \right)^{-3} \Big) + \left( \alpha t_o^3 \delta 2^{n+1} (n-1)n \right. \\
& \times (t_o (6\delta - 3) + 4\eta t) \left( \frac{6\eta^2}{t_o^2} + \frac{12\delta\eta}{t_o t} + \frac{3\delta(2\delta - 1)}{t^2} \right)^n \\
& \times \left. \left( t_o^2 \delta (2\delta - 1) + 4t_o \delta \eta t + 2\eta^2 t^2 \right)^{-2} \right)
\end{aligned}$$

$$- \frac{27\beta\mathcal{C}^4(t_o\delta + \eta t)^8}{64\pi^2 t_o^4 t^4 \left(\pi\alpha t_o^2 t^2 + (t_o\delta + \eta t)^2\right)^2} \Big]. \quad (48)$$

The EoS parameter for DE turns out to be

$$\begin{aligned}
\omega_{DE} = & \frac{64}{3} \left[ - \frac{144\alpha\delta(n-1)n(t_o\delta + \eta t)(t_o(2\delta-1) + 2\eta t)}{t_o^2 t^4} \right. \\
& + \alpha 3^{n+1} \left( \frac{4\eta^2}{t_o^2} + \frac{8\delta\eta}{t_o t} + \frac{2\delta(2\delta-1)}{t^2} \right)^n \\
& - \alpha 3^{n+1} n \left( \frac{4\eta^2}{t_o^2} + \frac{8\delta\eta}{t_o t} + \frac{2\delta(2\delta-1)}{t^2} \right)^n + \left( \alpha t_o^4 \delta^2 2^{n+2} (n-2) \right. \\
& \times (n-1)n(-2t_o\delta + t_o - 2\eta t)^2 \left( \frac{6\eta^2}{t_o^2} + \frac{12\delta\eta}{t_o t} + \frac{3\delta(2\delta-1)}{t^2} \right)^n \\
& \times \left( t_o^2 \delta(2\delta-1) + 4\delta\eta t_o t + 2\eta^2 t^2 \right)^{-3} + \left( \alpha t_o^3 \delta 2^{n+1} (n-1)n \right. \\
& \times (t_o(6\delta-3) + 4\eta t) \left( \frac{6\eta^2}{t_o^2} + \frac{12\delta\eta}{t_o t} + \frac{3\delta(2\delta-1)}{t^2} \right)^n \\
& \times \left( t_o^2 \delta(2\delta-1) + 4t_o \delta \eta t + 2\eta^2 t^2 \right)^{-2} \\
& - \frac{27\beta\mathcal{C}^4(t_o\delta + \eta t)^8}{64\pi^2 t_o^4 t^4 \left(\pi\alpha t_o^2 t^2 + (t_o\delta + \eta t)^2\right)^2} \Big] \left[ \alpha 2^{n+6} \left( \frac{6\eta^2}{t_o^2} \right. \right. \\
& + \frac{12\delta\eta}{t_o t} + \frac{3\delta(2\delta-1)}{t^2} \Big)^n - \alpha 2^{n+6} n \left( \frac{6\eta^2}{t_o^2} + \frac{12\delta\eta}{t_o t} + \frac{3\delta(2\delta-1)}{t^2} \right)^n \\
& + \frac{9\beta\mathcal{C}^4(t_o\delta + \eta t)^8}{\pi^2 t_o^4 t^4 \left(\pi\alpha t_o^2 t^2 + (t_o\delta + \eta t)^2\right)^2} + \left( \alpha t_o^2 \delta 2^{n+7} (n-1)n \right. \\
& \times (t_o\delta + \eta t)(t_o(2\delta-1) + 2\eta t) \left( \frac{6\eta^2}{t_o^2} + \frac{12\delta\eta}{t_o t} + \frac{3\delta(2\delta-1)}{t^2} \right)^n \\
& \times \left( t_o^2 \delta(2\delta-1) + 4\delta\eta t_o t + 2\eta^2 t^2 \right)^{-2} + \left( 6\mathcal{C}^2(t_o\delta + \eta t)^4 \left( \pi\alpha t_o^2 \right. \right. \\
& \times (-2^{n+2}) n t^2 \left( \frac{6\eta^2}{t_o^2} + \frac{12\delta\eta}{t_o t} + \frac{3\delta(2\delta-1)}{t^2} \right)^{n-1} \left( t_o^2 (\delta^2 + \pi\alpha t^2) \right.
\end{aligned}$$

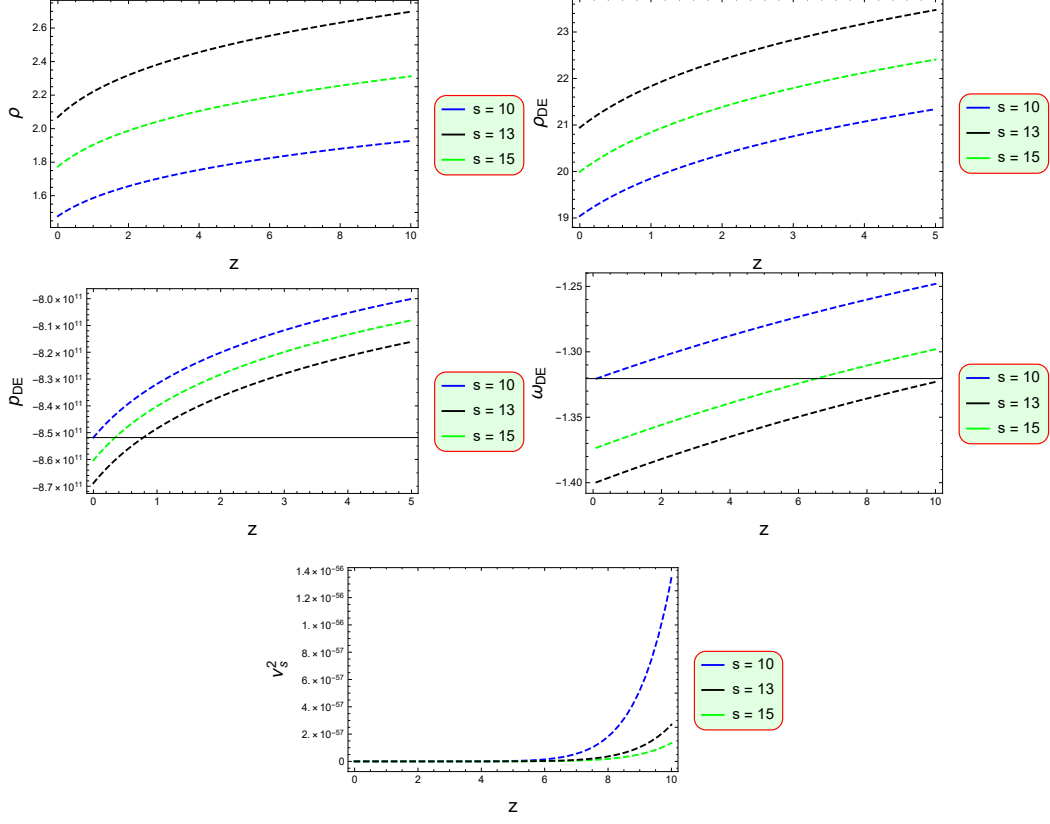


Figure 7: Parametric behavior of  $\rho$ ,  $\rho_{DE}$ ,  $p_{DE}$ ,  $\omega_{DE}$  and  $\nu_s^2$ .

$$\begin{aligned}
 & + 2t_o\delta\eta t + \eta^2 t^2) + 8\pi t_o^2 t^2 (\pi\alpha t_o^2 t^2 + (t_o\delta + \eta t)^2) + 3\beta\mathcal{C}^2 \\
 & \times (t_o\delta + \eta t)^4) \Big) \left( \pi^2 t_o^4 t^4 (\pi\alpha t_o^2 t^2 + (t_o\delta + \eta t)^2)^2 \right)^{-1} \Big]^{-1}. \quad (49)
 \end{aligned}$$

Figure 7 signifies that the energy density for RHDE is positive, suggesting accelerated cosmic expansion. This accelerated expansion is verified by the behavior of matter variables for DE, as energy density is positive and pressure is negative. The EoS parameter represents the phantom dominated era and stability analysis ensures a stable accelerating universe.

## 4.2 Sharma-Mittal Holographic Dark Energy Model

The Sharma-Mittal HDE density associated with the Riici horizon is derived using Eq. (36) and the expression for the Ricci horizon as

$$\rho_{SMDE} = \frac{3\mathcal{C}^2}{\mathcal{B}} \left( \frac{\delta\eta}{t_o} + \frac{\delta(\delta t - \beta)}{t^2} \right)^2 \left( \frac{\pi\chi}{\frac{\delta\eta}{t_o} + \frac{\delta(\delta t - \beta)}{t^2}} + 1 \right)^{\mathcal{B}\chi} - 1. \quad (50)$$

Using Eqs.(25), (28) and (50) into Eqs.(14) and (15), the expression for energy density and pressure for DE turn out to be

$$\begin{aligned} \rho_{DE} &= \frac{2^{-n}3^{1-n}}{\alpha n} \left( \frac{2\eta^2}{\mathcal{B}^2} + \frac{4\delta\eta}{\mathcal{B}t} + \frac{\delta(2\delta - 1)}{t^2} \right)^{1-n} \\ &\times \left[ \alpha 6^n \left( \frac{2\eta^2}{\mathcal{B}^2} + \frac{4\delta\eta}{\mathcal{B}t} + \frac{\delta(2\delta - 1)}{t^2} \right)^n \right. \\ &- \left. \alpha 6^n n \left( \frac{2\eta^2}{\mathcal{B}^2} + \frac{4\delta\eta}{\mathcal{B}t} + \frac{\delta(2\delta - 1)}{t^2} \right)^n \right. \\ &+ \left. \frac{\beta \left( t_o^2 \mathcal{B}t^4 - 3\mathcal{C}^2 \delta^2 \left( -t_o\beta + t_o\delta t + \eta t^2 \right)^2 \left( \frac{\pi\chi}{\frac{\delta\eta}{t_o} + \frac{\delta(\delta t - \beta)}{t^2}} + 1 \right)^{\mathcal{B}\chi} \right)^2}{t_o^4 \mathcal{B}^2 t^8} \right. \\ &+ \left. \left( \alpha t_o^2 \delta 2^{n+1} (n-1) n (t_o\delta + \eta t) (t_o(2\delta - 1) + 2\eta t) \right. \right. \\ &\times \left. \left( \frac{6\eta^2}{t_o^2} + \frac{12\delta\eta}{t_o t} + \frac{3\delta(2\delta - 1)}{t^2} \right)^n \right) \\ &\times \left. \left( t_o^2 \delta (2\delta - 1) + 4b\delta\eta t + 2\eta^2 t^2 \right)^{-2} \right. \\ &- \left. \left( t_o^2 \mathcal{B}t^4 - 3\mathcal{C}^2 \delta^2 \left( -t_o\beta + t_o\delta t + \eta t^2 \right)^2 \right. \right. \\ &\times \left. \left( \frac{\pi t_o t^2 \chi}{\delta \left( -t_o\beta + t_o\delta t + \eta t^2 \right)} + 1 \right)^{\mathcal{B}\chi} \right. \\ &\times \left. \left( t_o^2 \mathcal{B}t^4 - \alpha t_o^2 \mathcal{B} 6^{n-1} n t^4 \left( \frac{2\eta^2}{t_o^2} + \frac{4\delta\eta}{t_o t} + \frac{\delta(2\delta - 1)}{t^2} \right)^{n-1} \right. \right. \\ &- \left. \left. \beta \left( \mathcal{B} t_o^2 t^4 - 3\mathcal{C}^2 \delta^2 \left( -t_o\beta + t_o\delta t + \eta t^2 \right)^2 \right) \right. \right. \end{aligned}$$

$$\times \left( \frac{\pi t_o t^2 \chi}{\delta \left( -t_o \beta + t_o \delta t + \eta t^2 \right)} + 1 \right)^{\mathcal{B}\chi} \right) \left( t_o^4 \mathcal{B}^2 t^8 \right)^{-1} \Big]. \quad (51)$$

$$\begin{aligned}
p_{DE} &= \frac{6^{-n} \left( \frac{2\eta^2}{t_o^2} + \frac{4\delta\eta}{t_o t} + \frac{\delta(2\delta-1)}{t^2} \right)^{1-n}}{\alpha n} \\
&\times \left[ - \frac{144\alpha\delta(n-1)n(t_o\delta + \eta t)(t_o(2\delta-1) + 2\eta t)}{t_o^2 t^4} \right. \\
&+ \left( \alpha t_o^4 \delta^2 2^{n+2} (n-2)(n-1)n(b(2\delta-1) + 2\eta t)^2 \right. \\
&\times \left( \frac{6\eta^2}{t_o^2} + \frac{12\delta\eta}{t_o t} + \frac{3\delta(2\delta-1)}{t^2} \right)^n \\
&\times \left( t_o^2 \delta(2\delta-1) + 4t_o \delta \eta t + 2\eta^2 t^2 \right)^{-3} \\
&+ \left( \alpha t_o^3 \delta 2^{n+1} (n-1)n(t_o(6\delta-3) + 4\eta t) \right. \\
&\times \left( \frac{6\eta^2}{t_o^2} + \frac{12\delta\eta}{t_o t} + \frac{3\delta(2\delta-1)}{t^2} \right)^n \\
&\times \left( t_o^2 \delta(2\delta-1) + 4t_o \delta \eta t + 2\eta^2 t^2 \right)^{-2} \\
&+ \frac{3}{t_o^4 \mathcal{B}^2 t^8} \left( \alpha b^4 \mathcal{B}^2 6^n t^8 \left( \frac{2\eta^2}{t_o^2} + \frac{4\delta\eta}{t_o t} + \frac{\delta(2\delta-1)}{t_o^2 t^2} \right)^n \right. \\
&- \left. \alpha t_o^4 \mathcal{B}^2 6^n n t^8 \left( \frac{2\eta^2}{t_o^2} + \frac{4\delta\eta}{t_o t} + \frac{\delta(2\delta-1)}{t^2} \right)^n \right. \\
&- \left. \beta \left( t_o^2 \mathcal{B} t^4 - 3\mathcal{C}^2 \delta^2 \left( -t_o \beta + t_o \delta t_o t + \eta t_o^2 t^2 \right)^2 \right) \right. \\
&\times \left. \left( \frac{\pi \chi}{\frac{\delta\eta}{t_o} + \frac{\delta(\delta t - \beta)}{t^2}} + 1 \right)^{\mathcal{B}\chi} \right)^2 \Big) \Big] \quad (52)
\end{aligned}$$

The EoS parameter for SMHDE model associated with Ricci horizon is given as

$$\omega_{DE} = \left[ - \frac{144\alpha\delta(n-1)n(t_o\delta + \eta t)(t_o(2\delta-1) + 2\eta t)}{t_o^2 t^4} \right.$$

$$\begin{aligned}
& + \left( \alpha t_o^4 \delta^2 2^{n+2} (n-2)(n-1)n(t_o(2\delta-1) + 2\eta t)^2 \right. \\
& \times \left( \frac{6\eta^2}{t_o^2} + \frac{12\delta\eta}{t_o t} + \frac{3\delta(2\delta-1)}{t^2} \right)^n \Big) \\
& \times \left( t_o^2 \delta(2\delta-1) + 4\delta\eta t t_o + 2\eta^2 t^2 \right)^{-3} \\
& + \left( \alpha t_o^3 \delta 2^{n+1} (n-1)n(t_o(6\delta-3) + 4\eta t) \right. \\
& \times \left( \frac{6\eta^2}{t_o^2} + \frac{12\delta\eta}{t_o t} + \frac{3\delta(2\delta-1)}{t^2} \right)^n \Big) \\
& \times \left( t_o^2 \delta(2\delta-1 + 4t_o\delta\eta t + 2\eta^2 t^2) \right)^{-2} \\
& + \frac{3}{t_o^4 \mathcal{B}^2 t^8} \left( \alpha t_o^4 \mathcal{B}^2 6^n t^8 \left( \frac{2\eta^2}{t_o^2} + \frac{4\delta\eta}{t_o t} + \frac{\delta(2\delta-1)}{t^2} \right)^n \right. \\
& - \left. \alpha t_o^4 \mathcal{B}^2 6^n n t^8 \left( \frac{2\eta^2}{t_o^2} + \frac{4\delta\eta}{t_o t} + \frac{\delta(2\delta-1)}{t^2} \right)^n \right. \\
& - \left. \beta \left( t_o^2 \mathcal{B} t^4 - 3\mathcal{C}^2 \delta^2 \left( -t_o\beta + t_o\delta t + \eta t^2 \right)^2 \right. \right. \\
& \times \left. \left. \left( \frac{\pi\chi}{\frac{\delta\eta}{t_o} + \frac{\delta(\delta t - \beta)}{t^2}} + 1 \right)^{\mathcal{B}\chi} \right)^2 \right) \Big] \\
& \times \left[ \alpha 6^n \left( \frac{2\eta^2}{\mathcal{B}^2} + \frac{4\delta\eta}{\mathcal{B} t} + \frac{\delta(2\delta-1)}{t^2} \right)^n \right. \\
& - \left. \alpha 6^n n \left( \frac{2\eta^2}{\mathcal{B}^2} + \frac{4\delta\eta}{\mathcal{B} t} + \frac{\delta(2\delta-1)}{t^2} \right)^n \right. \\
& + \left. \frac{\beta \left( t_o^2 \mathcal{B} t^4 - 3\mathcal{C}^2 \delta^2 \left( -t_o\beta + t_o\delta t + \eta t^2 \right)^2 \left( \frac{\pi\chi}{\frac{\delta\eta}{t_o} + \frac{\delta(\delta t - \beta)}{t^2}} + 1 \right)^{\mathcal{B}\chi} \right)^2}{t_o^4 \mathcal{B}^2 t^8} \right. \\
& + \left. \left( \alpha t_o^2 \delta 2^{n+1} (n-1)n(t_o\delta + \eta t)(t_o(2\delta-1) + 2\eta t) \right. \right. \\
& \times \left. \left. \left( \frac{6\eta^2}{t_o^2} + \frac{12\delta\eta}{t_o t} + \frac{3\delta(2\delta-1)}{t^2} \right)^n \right) \right]
\end{aligned}$$

$$\begin{aligned}
& \times \left( t_o^2 \delta(2\delta - 1) + 4t_o \delta \eta t + 2\eta^2 t^2 \right)^{-2} \\
& - \left( t_o^2 \mathcal{B} t^4 - 3\mathcal{C}^2 \delta^2 \left( -t_o \beta + t_o \delta t + \eta t^2 \right)^2 \right. \\
& \times \left( \frac{\pi t_o t^2 \chi}{\delta \left( -t_o \beta + t_o \delta t + \eta t^2 \right)} + 1 \right)^{\mathcal{B} \chi} \\
& \times \left( t_o^2 \mathcal{B} t^4 - \alpha t_o^2 \mathcal{B} 6^{n-1} n t^4 \left( \frac{2\eta^2}{t_o^2} + \frac{4\delta\eta}{t_o t} + \frac{\delta(2\delta-1)}{t^2} \right)^{n-1} \right. \\
& - \beta \left( t_o^2 \mathcal{B} t^4 - 3\mathcal{C}^2 \delta^2 \left( -t_o \beta + t_o \delta t + \eta t^2 \right)^2 \right. \\
& \times \left. \left. \left( \frac{\pi t_o t^2 \chi}{\delta \left( -t_o \beta + t_o \delta t + \eta t^2 \right)} + 1 \right)^{\mathcal{B} \chi} \right) \right) \left( t_o^4 \mathcal{B}^2 t^8 \right)^{-1} \Big]. \quad (53)
\end{aligned}$$

The graphical analysis presented in Figure 8 determines an accelerated expansion of the universe, characterized by a positive energy density and behavior of matter variables for DE. The trajectories of the EoS parameter indicate a quintessence era of DE and the squared sound speed parameter confirms the stability of the model.

### 4.3 Generalized Holographic Dark Energy Model

The expression for the GHDE for the Ricci horizon is given as

$$\rho_{GHDE} = \frac{3\mathcal{C}^2}{8\pi\mathcal{B}} \left( \frac{\delta\eta}{t_o} + \frac{\delta(\delta t - \beta)}{t^2} \right) \left( \left( \frac{\pi\alpha}{\lambda \left( \frac{\delta\eta}{t_o} + \frac{\delta(\delta t - \beta)}{t^2} \right)} + 1 \right)^\lambda - 1 \right). \quad (54)$$

The energy density and pressure for this DE model are obtained using Eq.(54) and Eq.(28) into Eqs.(14) and (15) as

$$\begin{aligned}
\rho_{DE} &= \frac{2^{-n-6} 3^{1-n} \left( \frac{2\eta^2}{t_o^2} + \frac{4\delta\eta}{t_o t} + \frac{\delta(2\delta-1)}{t^2} \right)^{1-n}}{\pi^2 \alpha t_o^2 \mathcal{B}^2 n t^4} \\
&\times \left[ \left( \pi^2 \alpha t_o^4 \mathcal{B}^2 \delta 2^{n+7} (n-1) n t^4 (t_o \delta + \eta t_o) (t_o (2\delta - 1) \right. \right.
\end{aligned}$$

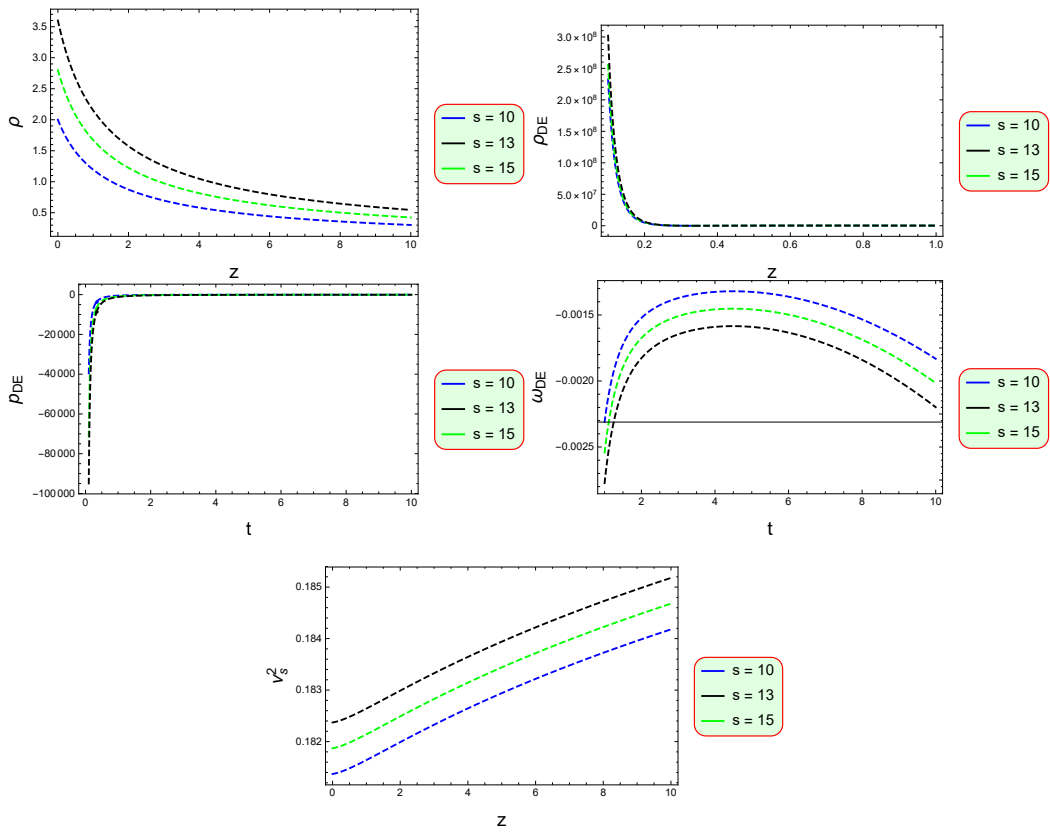


Figure 8: Parametric evolution of  $\rho$ ,  $\rho_{DE}$ ,  $p_{DE}$ ,  $\omega_{DE}$  and  $\nu_s^2$ .

$$\begin{aligned}
& + 2\eta t) \left( \frac{6\eta^2}{t_o^2} + \frac{12\delta\eta}{t_o t} + \frac{3\delta(2\delta-1)}{t^2} \right)^n \Big) \\
& \times \left( t_o^2 \delta(2\delta-1) + 4t_o \delta\eta t + 2\eta^2 t^2 \right)^{-2} \\
& + t_o^2 \left( \pi^2 \alpha \mathcal{B}^2 (-2^{n+6}) (n-1) t^4 \left( \frac{6\eta^2}{t_o^2} + \frac{12\delta\eta}{t_o t} \right. \right. \\
& + \left. \left. \frac{3\delta(2\delta-1)}{t^2} \right)^n + 9\beta \mathcal{C}^4 \delta^2 (\beta - \delta t)^2 \left( \left( \frac{\pi\alpha}{\lambda \left( \frac{\delta\eta}{t_o} + \frac{\delta(\delta t - \beta)}{t^2} \right)} \right. \right. \right. \\
& + \left. \left. \left. 1 \right)^\lambda - 1 \right)^2 \Big) + 6\mathcal{C}^2 \delta (t_o (\beta - \delta t) - \eta t^2) + 6\mathcal{C}^2 \delta (t_o (\beta - \delta t) - \eta t^2) \\
& \times 8\pi b \mathcal{B} t^2 - 3\mathcal{C}^2 \beta \delta (t_o (\beta - \delta t) - \eta t^2) \left( \left( \frac{\pi\alpha}{\lambda \left( \frac{\delta\eta}{t_o} + \frac{\delta(\delta t - \beta)}{t^2} \right)} \right. \right. \\
& + \left. \left. 1 \right)^\lambda - 1 \right) \left( 1 - \left( \frac{\pi\alpha}{\lambda \left( \frac{\delta\eta}{t_o} + \frac{\delta(\delta t - \beta)}{t^2} \right)} + 1 \right)^\lambda \right. \\
& - \left. \left. \frac{\pi\alpha t_o^3 \mathcal{B} 2^{n+2} 3^{n-1} n t^4 \left( \frac{2\eta^2}{t_o^2} + \frac{4\delta\eta}{t_o t} + \frac{\delta(2\delta-1)}{t^2} \right)^n}{t_o^2 \delta(2\delta-1) + 4t_o \delta\eta t + 2\eta^2 t^2} \right) \right. \\
& + 18t_o \beta \mathcal{C}^4 \delta^2 \eta t^2 (\delta t - \beta) \left( \left( \frac{\pi\alpha}{\lambda \left( \frac{\delta\eta}{t_o} + \frac{\delta(\delta t - \beta)}{t^2} \right)} + 1 \right)^\lambda - 1 \right)^2 \\
& + 9\beta \mathcal{C}^4 \delta^2 \eta^2 t^4 \left( \left( \frac{\pi\alpha}{\lambda \left( \frac{\delta\eta}{t_o} + \frac{\delta(\delta t - \beta)}{t^2} \right)} + 1 \right)^\lambda - 1 \right)^2. \tag{55}
\end{aligned}$$

$$\begin{aligned}
p_{DE} & = \frac{2^{-n-6} 3^{-n} \left( \frac{2\eta^2}{t_o^2} + \frac{4\delta\eta}{t_o t} + \frac{\delta(2\delta-1)}{t^2} \right)^{1-n}}{\alpha t_o^2 n} \\
& \times \left[ - \frac{9216 \alpha \delta (n-1) n (t_o \delta + \eta t) (t_o (2\delta-1) + 2\eta t)}{t^4} \right]
\end{aligned}$$

$$\begin{aligned}
& + 18t_o\beta\mathcal{C}^4\delta^2\eta t^2(\delta t - \beta) \left( \left( \frac{\pi\alpha}{\lambda \left( \frac{\delta\eta}{t_o} + \frac{\delta(\delta t - \beta)}{t^2} \right)} + 1 \right)^\lambda - 1 \right)^2 \\
& + 9\beta\mathcal{C}^4\delta^2\eta^2t^4 \left( \left( \frac{\pi\alpha}{\lambda \left( \frac{\delta\eta}{t_o} + \frac{\delta(\delta t - \beta)}{t^2} \right)} + 1 \right)^\lambda - 1 \right)^2 \\
& + 9\beta\mathcal{C}^4\delta^2(\beta - \delta t)^2 \left( \left( \frac{\pi\alpha}{\lambda \left( \frac{\delta\eta}{t_o} + \frac{\delta(\delta t - \beta)}{t^2} \right)} + 1 \right)^\lambda - 1 \right)^2 \\
& - \frac{1}{\pi^2\mathcal{B}^2t^4} 3 \left( t_o^2 \left( \pi^2\alpha\mathcal{B}^22^{n+6}(n-1)t^4 \left( \frac{6\eta^2}{t_o^2} + \frac{12\delta\eta}{t_o t} \right. \right. \right. \\
& + \left. \left. \left. \frac{3\delta(2\delta-1)}{t^2} \right)^n \right) \right) + \left( \alpha t_o^6\delta^22^{n+8}(n-2)(n-1)n(t_o(2\delta-1) \right. \\
& + 2\eta t)^2 \left( \frac{6\eta^2}{t_o^2} + \frac{12\delta\eta}{t_o t} + \frac{3\delta(2\delta-1)}{t^2} \right)^n \left( t_o^2\delta(2\delta-1) + 4t_o\delta\eta t \right. \\
& + 2\eta^2t^2 \left. \right)^{-3} \left. \right) + \left( \alpha t_o^5\delta^22^{n+7}(n-1)n(t_o(6\delta-3) + 4\eta t) \right. \\
& \times \left( \frac{6\eta^2}{t_o^2} + \frac{12\delta\eta}{t_o t} + \frac{3\delta(2\delta-1)}{t^2} \right)^n \left( t_o^2\delta(2\delta-1) + 4t_o\delta\eta t \right. \\
& + 2\eta^2t^2 \left. \right)^{-2} \left. \right). \tag{56}
\end{aligned}$$

The EoS parameter turns out to be

$$\begin{aligned}
\omega_{DE} &= \left[ \pi^2\mathcal{B}^2t^4 \left( - \frac{9216\alpha\delta(n-1)n(t_o\delta + \eta t)(t_o(2\delta-1) + 2\eta t)}{t^4} \right. \right. \\
&+ \left( \alpha t_o^6\delta^22^{n+8}(n-2)(n-1)n(t_o(2\delta-1) + 2\eta t)^2 \right. \\
&\times \left( \frac{6\eta^2}{t_o^2} + \frac{12\delta\eta}{t_o t} + \frac{3\delta(2\delta-1)}{t^2} \right)^n \left( t_o^2\delta(2\delta-1) + 4t_o\delta\eta t \right. \\
&+ 2\eta^2t^2 \left. \right)^{-3} + \left( \alpha t_o^5\delta^22^{n+7}(n-1)n(t_o(6\delta-3) + 4\eta t) \right. \\
&\times \left. \left( \frac{6\eta^2}{t_o^2} + \frac{12\delta\eta}{t_o t} + \frac{3\delta(2\delta-1)}{t^2} \right)^n \right) \left( t_o^2\delta(2\delta-1) + 4t_o\delta\eta t \right. \\
&+ 2\eta^2t^2 \left. \right)^{-2} \left. \right]. 
\end{aligned}$$

$$\begin{aligned}
& + 2\eta^2 t^2 \Big)^{-2} \Big) - \frac{3}{\pi^2 \mathcal{B}^2 t^4} \left( t_{\circ}^2 \left( \pi^2 \alpha \mathcal{B}^2 2^{n+6} (n-1) t^4 \left( \frac{6\eta^2}{t_{\circ}^2} + \frac{12\delta\eta}{t_{\circ} t} \right. \right. \right. \\
& + \left. \left. \left. \frac{3\delta(2\delta-1)}{t^2} \right)^n \right) \right) + \left( \alpha t_{\circ}^6 \delta^2 2^{n+8} (n-2)(n-1)n(t_{\circ}(2\delta-1) \right. \\
& + \left. 2\eta t)^2 \left( \frac{6\eta^2}{t_{\circ}^2} + \frac{12\delta\eta}{t_{\circ} t} + \frac{3\delta(2\delta-1)}{t^2} \right)^n \left( t_{\circ}^2 \delta(2\delta-1) + 4t_{\circ} \delta\eta t \right. \right. \\
& + \left. \left. 2\eta^2 t^2 \right)^{-3} \right) + 18t_{\circ} \beta \mathcal{C}^4 \delta^2 \eta t^2 (\delta t - \beta) \left( \left( \frac{\pi\alpha}{\lambda \left( \frac{\delta\eta}{t_{\circ}} + \frac{\delta(\delta t - \beta)}{t^2} \right)} + 1 \right)^{\lambda} - 1 \right)^2 \\
& + \left. 9\beta \mathcal{C}^4 \delta^2 \eta^2 t^4 \left( \left( \frac{\pi\alpha}{\lambda \left( \frac{\delta\eta}{t_{\circ}} + \frac{\delta(\delta t - \beta)}{t^2} \right)} + 1 \right)^{\lambda} - 1 \right)^2 \right) \Big] \\
& \times \left[ 3 \left( \left( \pi^2 \alpha t_{\circ}^4 \mathcal{B}^2 \delta 2^{n+7} (n-1) n t^4 (t_{\circ} \delta + \eta t) (t_{\circ} (2\delta-1) \right. \right. \right. \\
& + \left. \left. \left. 2\eta t) \left( \frac{6\eta^2}{t_{\circ}^2} + \frac{12\delta\eta}{t_{\circ} t} + \frac{3\delta(2\delta-1)}{t^2} \right)^n \right) \right. \\
& \times \left. \left. \left. \left( t_{\circ}^2 \delta(2\delta-1) + 4t_{\circ} \delta\eta t + 2\eta^2 t^2 \right)^{-2} \right. \right. \right. \\
& + \left. \left. \left. t_{\circ}^2 \left( \pi^2 \alpha \mathcal{B}^2 (-2^{n+6}) (n-1) t^4 \left( \frac{6\eta^2}{t_{\circ}^2} + \frac{12\delta\eta}{t_{\circ} t} \right. \right. \right. \right. \\
& + \left. \left. \left. \left. \frac{3\delta(2\delta-1)}{t^2} \right)^n + 9\beta \mathcal{C}^4 \delta^2 (\beta - \delta t)^2 \left( \left( \frac{\pi\alpha}{\lambda \left( \frac{\delta\eta}{t_{\circ}} + \frac{\delta(\delta t - \beta)}{t^2} \right)} + 1 \right)^{\lambda} - 1 \right)^2 \right. \right. \right. \\
& + \left. \left. \left. 1 \right)^{\lambda} - 1 \right)^2 \right) + 6\mathcal{C}^2 \delta (t_{\circ} (\beta - \delta t) - \eta t^2) + 6\mathcal{C}^2 \delta (t_{\circ} (\beta - \delta t) - \eta t^2) \right. \\
& \times \left. 8\pi t_{\circ} \mathcal{B} t^2 - 3\mathcal{C}^2 \beta \delta (t_{\circ} (\beta - \delta t) - \eta t^2) \left( \left( \frac{\pi\alpha}{\lambda \left( \frac{\delta\eta}{t_{\circ}} + \frac{\delta(\delta t - \beta)}{t^2} \right)} + 1 \right)^{\lambda} - 1 \right) \right. \\
& + \left. \left. \left. 1 \right)^{\lambda} - 1 \right) \left( 1 - \left( \frac{\pi\alpha}{\lambda \left( \frac{\delta\eta}{t_{\circ}} + \frac{\delta(\delta t - \beta)}{t^2} \right)} + 1 \right)^{\lambda} \right)
\end{aligned}$$

$$\begin{aligned}
& - \frac{\pi\alpha t_o^3 \mathcal{B} 2^{n+2} 3^{n-1} n t^4 \left( \frac{2\eta^2}{t_o^2} + \frac{4\delta\eta}{t_o t} + \frac{\delta(2\delta-1)}{t^2} \right)^n}{t_o^2 \delta(2\delta-1) + 4t_o \delta\eta t + 2\eta^2 t^2} \\
& + 18t_o \beta \mathcal{C}^4 \delta^2 \eta t^2 (\delta t - \beta) \left( \left( \frac{\pi\alpha}{\lambda \left( \frac{\delta\eta}{t_o} + \frac{\delta(\delta t - \beta)}{t^2} \right)} + 1 \right)^\lambda - 1 \right)^2 \\
& + 9\beta \mathcal{C}^4 \delta^2 \eta^2 t^4 \left( \left( \frac{\pi\alpha}{\lambda \left( \frac{\delta\eta}{t_o} + \frac{\delta(\delta t - \beta)}{t^2} \right)} + 1 \right)^\lambda - 1 \right)^2 \Big]^{-1}. \tag{57}
\end{aligned}$$

Figure 9 demonstrates the cosmological evolution of the energy density, pressure, EoS parameter and squared sound speed parameter, which collectively describe the stable cosmic accelerated expansion.

## 5 Conclusions

Modified gravity theories have emerged as essential frameworks for addressing the limitations of GR. Among these,  $f(R, T^2)$  gravity provides a novel extension by incorporating nonlinear contributions of the trace of the energy-momentum tensor. This extension allows for a more refined description of matter-energy interactions, offering deep insights into cosmic evolution. By incorporating self contraction of stress energy tensor  $T^2$ , this theory gives a significant understanding of how matter fields effects gravitational dynamics. This inclusion plays a comprehensive role in studying the complexities of energy exchanges between DE, dark matter and ordinary matter. Consequently, the study of EMSG is pivotal in exploring our understanding of fundamental relations between matter and gravity.

In this manuscript, we have studied the cosmic dynamics by exploring the RHDE, SHMDE and GHDE models for Hubble horizon and Ricci horizon as IR cutoff in the background of EMSG. To achieve a deep understanding of cosmic evolution, we have calculated key cosmological parameters including scale factor, Hubble parameter, deceleration parameter and EoS parameter. By exploring these parameters along with the matter variables we have demonstrated how these variants of HDE models explain the cosmic accelerated expansion. Our study gives a comprehensive understanding of the cosmic evolution, offering important findings on the behavior of DE and its

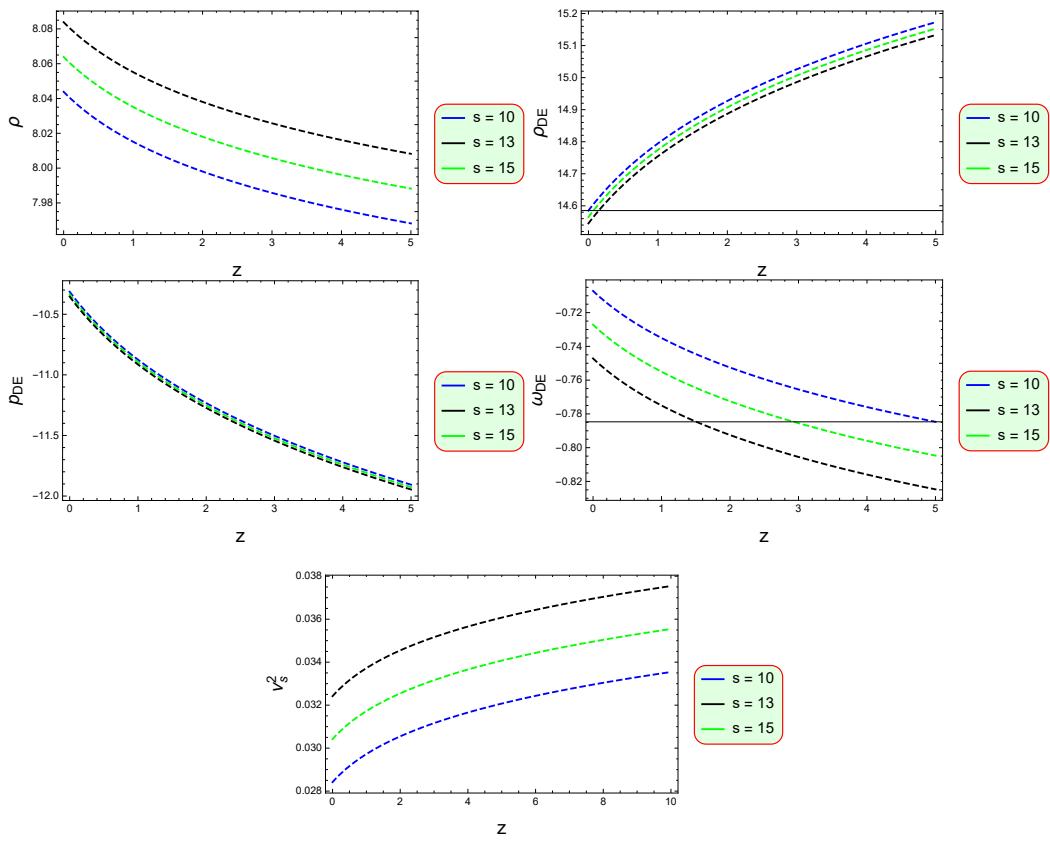


Figure 9: Parametric behavior of  $\rho$ ,  $\rho_{DE}$ ,  $p_{DE}$ ,  $\omega_{DE}$  and  $\nu_s^2$ .

role on the cosmic accelerated expansion. The key finding of our analysis as follows.

The scale factor and Hubble parameter show positive values, this refers accelerated cosmic expansion. The negative deceleration parameter confirms the accelerated expansions which occur at later times. The Hubble parameter as a function of redshift  $H(z)$  agrees with the Planck observation data and mimics geometric DE, without the need of cosmological constant in  $\Lambda$ CDM, this overcomes the fine-tuning problem [65] (Figure 1). There are slight discrepancies at the redshifts where  $(1 < z < 2)$ . This reflects the influence of  $T^2$  and is consistent with DESI or Euclid. The energy density remains positive which supports role of the variant of HDE models in the cosmic accelerated expansion. The HDE models show adaptability for the various phases in cosmic acceleration. The EoS parameter significantly determines the phantom or quintessence behavior, illustrating the model adaptability in capturing different phases of cosmic acceleration. These variants of HDE models were found to be stable against perturbations through the squared sound speed parameter, ensuring its physical viability. These findings collectively suggest that these DE models are compelling candidate for examining the cosmic late-time accelerated expansion in EMSG.

Jawad et al [66] studied the cosmic accelerated expansion through the HDE models, their investigation did not perform the stability analysis of these models. However, our study gives a more significant analysis by determining that these DE models not only explain cosmic acceleration but also show stability through the squared sound speed parameter. Moreover, we determine a clear understanding of the EoS parameter, which transition from the phantom regime in the early cosmos to the quintessence era at late times, addressing the model's agreement with observational data. Furthermore, our results shows consistency with the work of Saleem and Ijaz [67], validating the robustness of our approach. By providing a more refined analysis of cosmic dynamics, including stability and the evolving nature of DE, our research offers an enhanced understanding of the universe accelerated expansion in the framework of  $f(R, T^2)$  gravity.

**Data Availability Statement:** No new data were generated or analyzed in support of this research.

**Credit Author Statement:** **M. Sharif:** Conceptualization, Supervision, Writing- Reviewing and Editing. **M. Zeeshan Gul:** Investigation, Formal

analysis. **Imran Hashim:** Methodology, Software, Writing- Original draft preparation.

## References

- [1] Buchdahl, H. A.: Mon. Not. R. Astron. Soc. **150**(1970)1.
- [2] Dolgov, A.D. and Kawasaki, M.: Phys. Lett. B **573**(2003)1; Capozziello, S., Cardone, V.F. and Troisi, A.: Phys. Rev. D **71**(2005)043503.
- [3] Adeel, M. et al.: Mod. Phys. Lett. A **38**(2023)2350152.
- [4] Rani, S. et al.: Int. J. Geom. Methods Mod. Phys. **21**(2024)2450033.
- [5] Waseem, A. et al.: Eur. Phys. J. C **83**(2023)1088.
- [6] Mustafa, G. et al.: Eur. Phys. J. C **84**(2023)690; Ann. Phys. **460**(2024)169551; Chin. J. Phys. **88**(2024)32
- [7] Asad, H. et al.: Phys. Dark Universe **46**(2024) 101666.
- [8] Nan G. et al.: Phys. Dark Universe **46**(2024)101635.
- [9] Yousaf, M. Asad, H.: Phys. Dark Universe **48**(2025)101841; Yousaf, M.: Chin. J. Phys. **95**(2025)1278.
- [10] Dai, E. et al.: Nucl. Phys. B **1018**(2025)117017; Bhatti, M.Z. et al.: Int. J. Geom. Methods Mod Phys. **0**(2025)2550209.
- [11] Nasir, M.M.M. et al.: Eur. Phys. J. C **85**(2025)159.
- [12] Javed, F. et al.: Ann. Phys. **476**(2025)169956.
- [13] Rehman, A. et al.: Eur. Phys. J. C **85**(2025)949; Farwa, U. Abass, A. and Yousaf, M.: Nucl. Phys. B **1018**(2025)117086.
- [14] Yousaf, M. et al.: Chin. J. Phys. **97**(2025)1284.
- [15] Javed, F. et al.: Nucl. Phys. B **1018**(2025)117001.
- [16] Javed, F. et al.: Ann. Phys. **482**(2025)170189.

- [17] Yousaf, M. Asad, H. and Rehman, A.: Phys. Dark Universe **48**(2025)101888.
- [18] Malik, A. et al.: Phys. Dark Universe **50**(2025)102114.
- [19] Rani, S. et al.: Phys. Dark Universe **47**(2025)101754.
- [20] Fatima, N. et al.: Nucl. Phys. B **1016**(2025)116923.
- [21] Rani, S. et al.: Mod. Phys. Lett. A **40**(2025)2450213.
- [22] Katirci, N. and Kavuk, M.: Eur. Phys. J. Plus **129**(2014)163.
- [23] Pandya, D.M., Thomas, V.O. and Sharma, R.: Astrophys. Space Sci. **356**(2015)292.
- [24] Roshan, M. and Shojai, F.: Phys. Rev. D **94**(2016)044002.
- [25] Board, C.V.R. and Barrow, J.D.: Phys. Rev. D **96**(2017)123517.
- [26] Akarsu, O., Katirci, N. and Kumar, S.: Phys. Rev. D **97**(2018)024011.
- [27] Nari, N. and Roshan, M.: Phys. Rev. D **98**(2018)024031.
- [28] Moraes, P.H.R.S. and Sahoo, P.K.: Phys. Rev. D **97**(2018)024007.
- [29] Bahamonde, S., Marciu, M. and Rudra, P.: Phys. Rev. D **100**(2019)083511.
- [30] Ranjit, C., Rudra, P. and Kundu, S.: Ann. Phys. **428**(2021)168432.
- [31] Gul, M.Z. et al.: Phys. Dark Universe **45**(2024)101537.
- [32] Sharif, M. et al.: Phys. Dark Universe **46**(2024)101606.
- [33] Gul, M.Z. et al.: Chin. J. Phys. **89**(2024)1347.
- [34] Sharif, M. et al.: Chin. J. Phys. **89**(2024)266.
- [35] Hashim, I. et al.: High Energy Density Phys. **57**(2025)101223.
- [36] Hashim, I. et al.: Int. J. Geom. Methods Mod. Phys. **22**(2025)2540049.
- [37] Chattopadhyay S. et al.: Astrophys. Space Sci. **353**(2014)27.

- [38] Jawad, A. and Rani, S.: *Astrophys. Space Sci.* **359**(2015)23.
- [39] Jawad, A. and Chattopadhyay, S.: *Astrophys. Space Sci.* **357**(2015)37.
- [40] Odintsov, S.D., Oikonomou, V.K. and Banerjee, S.: *Nucl. Phys. B* **938**(2019)935.
- [41] Chiba, T., Okabe, T. and Yamaguchi, M.: *Phys. Rev. D* **62**(2000)023511; Kamenshchik, A.Y., Moschella, U. and Pasquier, V.: *Phys. Lett. B* **511**(2001)265.
- [42] Li, M.: *Phys. Lett. B* **603**(2004)5.
- [43] Moradpour, H. et al.: *Eur. Phys. J. C* **78**(2018)6.
- [44] Tavayef, M. et al.: *Phys. Lett. B* **781**(2018)195.
- [45] Jahromi, A.S. et al.: *Phys. Lett. B* **780**(2018)21.
- [46] Jawad, A. et al.: *Symmetry* **10**(2018)635.
- [47] Moradpour, H. et al.: *Eur. Phys. J. C* **78**(2018)829.
- [48] Iqbal, A. and Jawad, A.: *Phys. Dark Universe* **26**(2019)100349.
- [49] Maity, S. and Debnath, U.: *Eur. Phys. J. Plus* **134**(2019)514.
- [50] Prasanthi, U.D. and Aditya, Y.: *Results Phys.* **17**(2020)103101.
- [51] Sharma, U.K. and Dubey, V.C.: *Eur. Phys. J. Plus* **135**(2020)391.
- [52] Bandyopadhyay, T. and Debnath, U.: *Mod. Phys. Lett. A* **36**(2021)2150081.
- [53] Shekh, S.H., Moraes, P.H. and Sahoo, P.K.: *Universe* **7**(2021)67.
- [54] Sardar, A. and Debnath, U.: *Mod. Phys. Lett. A* **36**(2021)2150180.
- [55] Nojiri, S.I., Odintsov, S.D. and Paul, T.: *Symmetry* **13**(2021)928.
- [56] Upadhyay, S. and Dubey, V.C.: *Gravit. Cosmol.* **27**(2021)281.
- [57] Aditya, Y. and Prasanthi, U.D.: *Bulg. Astron. J.* **38**(2023)52.

- [58] Aditya, Y., Tejeswararao, D. and Prasanthi, U.D.: *East Eur. J. Phys.* **1**(2024)85.
- [59] Gul, M.Z. et al.: *Astron. Comput.* **52**(2025)100956.
- [60] Gul, M.Z. et al.: *Eur. Phys. J. Plus* **140**(2025)18.
- [61] Sharif, M. et al.: *High Energy Density Phys.* **55**(2025)101185.
- [62] Gaztanaga, E., Bonvin, C. and Hui, L.: *J. Cosmol. Astropart. Phys.* **01**(2017)032.
- [63] Jiao, K., Borghi, N., Moresco, M. and Zhang, T.J.: *Astrophys. J. Suppl.* **265**(2023)48.
- [64] Cohen, A.G., Kaplan, D.B. and Nelson, A.E.: *Phys. Rev. Lett.* **82**(1999)4971.
- [65] Akrami, Y. et al.: *Astron. Astrophys.* **641**(2020)A10.
- [66] Jawad, A. et al.: *Symmetry*, **10**(2018)635.
- [67] Saleem, R., Ijaz, A. and Waheed, S.: *Fortschr. der Phys.* **73**(2025)2300276.